ZUFSP Deubiquitylates K63-Linked Polyubiquitin Chains to Promote Genome Stability

Haahr, Peter; Borgermann, Nikoline; Guo, Xiaohu; Typas, Dimitris; Achuthankutty, Divya; Hoffmann, Saskia; Shearer, Robert; Sixma, Titia K; Mailand, Niels

Published in:
Molecular Cell

DOI:
10.1016/j.molcel.2018.02.024

Publication date:
2018

Document version
Peer reviewed version

ZUFSP deubiquitylates K63-linked polyubiquitin chains to promote genome stability

Peter Haahr[1], Nikoline Borgermann[1], Xiaohu Guo[2], Dimitris Typas[1], Divya Achuthankutty[1,3], Saskia Hoffmann[1], Robert Shearer[1], Titia K. Sixma[2], Niels Mailand[1,3,4,*]

[1]Novo Nordisk Foundation Center for Protein Research, Faculty of Health and Medical Sciences, University of Copenhagen, Blegdamsvej 3B, 2200 Copenhagen, Denmark; [2]Division of Biochemistry, Cancer Genomics Center, Netherlands Cancer Institute, Amsterdam, Netherlands; [3]Center for Chromosome Stability, Faculty of Health and Medical Sciences, University of Copenhagen, Blegdamsvej 3B, 2200 Copenhagen, Denmark; [4]Lead Contact

[*]Correspondence: niels.mailand@cpr.ku.dk

Summary

Deubiquitylating enzymes (DUBs) enhance the dynamics of the versatile ubiquitin (Ub) code by reversing and regulating cellular ubiquitylation processes at multiple levels. Here, we discovered that the uncharacterized human protein ZUFSP (Zinc finger with UFM1-specific peptidase domain protein), which has been annotated as a potentially inactive UFM1 protease, and its fission yeast homologue Mug105 define a previously unrecognized class of evolutionarily conserved cysteine protease DUBs. Human ZUFSP selectively interacts with and cleaves long K63-linked poly-Ub chains by means of tandem Ub-binding domains, while it displays poor activity towards mono- or di-Ub substrates. In cells, ZUFSP is recruited to and regulates K63-Ub conjugates at genotoxic stress sites, promoting chromosome stability upon replication stress in a manner dependent on its catalytic activity. Our findings establish ZUFSP (ZUP1) as a new type of linkage-selective cysteine peptidase DUB with a role in genome maintenance pathways.

Introduction

Post-translational modifications of proteins by ubiquitin (Ub) play key regulatory roles in virtually all aspects of eukaryotic cell biology. Conjugation of Ub moieties to lysine residues in target proteins proceeds via a three-step cascade involving numerous E1, E2 and E3 enzymes, forming the basis of a complex Ub code that entails the modification of tens of thousands of individual sites distributed among a large number of substrates (Kim et al., 2011; Komander and Rape, 2012; Wagner et al., 2011). In addition to modifying other proteins, Ub can be conjugated to any of the seven internal lysine (K) residues or the N-terminal methionine within Ub itself, giving rise to eight distinct Ub chain linkages, all of which occur in cells and serve particular, albeit not in all cases well understood, functions (Elia et al., 2015; Komander and Rape, 2012; Kulathu and Komander, 2012). For instance, K11- and K48-linked Ub chains are major signals for proteasomal degradation, whereas K63-linked ubiquitylation is a non-proteolytic modification with critical regulatory roles in a range of key cellular processes including the DNA damage response (DDR), innate immunity and membrane trafficking (Chen and Sun, 2009; Jackson and Durocher, 2013; Komander and Rape, 2012; Wu and Karin, 2015). The functional outcome of individual Ub-dependent modifications is determined by a diverse range of cellular proteins harboring Ub-binding domains (UBDs), more than 20 types of which have been identified (Husnjak and Dikic, 2012). By recognizing particular Ub topologies via their UBDs, often in conjunction with direct interaction with the ubiquitylated ligand, these factors bind specific subsets of ubiquitylated proteins and link the modifications to appropriate effector pathways.

In addition to its versatility, protein ubiquitylation is a highly dynamic and reversible

modification, due in large part to the existence of deubiquitylating enzymes (DUBs), around 100 of which are encoded by mammalian genomes (Mevissen and Komander, 2017; Nijman et al., 2005). The majority of DUBs are cysteine proteases, comprising five distinct classes, while a small proportion belongs to the JAMM motif family of metalloproteases (Mevissen and Komander, 2017). Whereas many DUBs, including most members of the USP-type family, display little apparent selectivity for cleaving particular Ub chain topologies, a smaller subset including several JAMM and OTU family DUBs have a strong preference for hydrolysis of one or a few defined linkage types (Mevissen and Komander, 2017).

Besides Ub, eukaryotic cells encode around a dozen small Ub-like modifier proteins (UBLs), many of which play well-defined and important cellular roles (Hochstrasser, 2009; van der Veen and Ploegh, 2012). While the enzymatic cascades underlying attachment of most UBLs to target proteins are overall similar to the Ub conjugation machinery, they comprise far fewer enzymes and in most cases target a more narrow range of substrates. For instance, protein modification by UFM1, the cellular functions of which are not fully understood but include hematopoiesis and the endoplasmic reticulum stress response, appears to be catalyzed by single E1, E2 and E3 enzymes (Cai et al., 2015; Komatsu et al., 2004; Tatsumi et al., 2010; Tatsumi et al., 2011). Like DUBs, dedicated proteases for UFM1 and a number of other UBLs including SUMO, NEDD8 and ISG15 enable the reversibility of these modifications (Cope et al., 2002; Hickey et al., 2012; Kang et al., 2007; Malakhov et al., 2002).

Here, we report the surprising discovery that human ZUFSP, an uncharacterized cysteine peptidase protein annotated as a potential, but most likely inactive UFM1-

specific protease, is a DUB that selectively recognizes and cleaves long K63-linked poly-Ub chains to promote cellular responses to genotoxic stress. Our findings reveal the existence of a hitherto unrecognized type of evolutionarily conserved cysteine protease DUB that is distinct from the five known families of thiol DUBs, and whose catalytic activity has a role in maintaining chromosomal stability in human cells.

Results

ZUFSP is a cysteine protease DUB

Several proteins with important roles in Ub-mediated responses to DNA damage, including the E3 ligases RNF168 and RNF169, interact with Ub at DNA damage sites via the Motif Interacting with Ubiquitin (MIU) (Doil et al., 2009; Lee et al., 2006; Panier et al., 2012; Penengo et al., 2006; Poulsen et al., 2012; Stewart et al., 2009). Through *in silico* searches for other potential MIU-containing DDR factors, we noted that the uncharacterized human protein ZUFSP (Zinc finger with UFM1-specific peptidase domain protein/C6orf113) contains a highly conserved MIU motif in its central portion (Fig. 1A; see also Fig. 2C). The modular domain organization of ZUFSP additionally includes four adjacent N-terminal Zinc finger motifs (ZnF) and a C-terminal peptidase domain with similarity to the UFM1-specific proteases UFSP1/2 (Fig. 1A,B). Given that ZUFSP contains an MIU motif and co-purifies with RPA subunits (Tkac et al., 2016), we speculated that it might function in Ub-mediated genome maintenance pathways. Notably, while the ZUFSP peptidase domain shows similarity to established UFM1-specific proteases, it conspicuously lacks the catalytic histidine residue present in these proteins (Fig. 1B, red arrow) (Ha et al., 2011), and is therefore thought to be catalytically inactive. However, ZUFSP contains adjacent,

conserved His residues that could serve a catalytic function (Fig. 1B, green arrows), and given the presence of a potential MIU motif, we reasoned that ZUFSP might be a DUB. In support of this hypothesis, we found that human ZUFSP readily interacted with immobilized Ub (Fig. S1A). To begin to address whether ZUFSP has intrinsic DUB activity, we assayed for covalent trapping of ZUFSP by a vinyl sulfone (VS)-Ub probe, which irreversibly reacts with the active site cysteines present in most DUBs (Ovaa, 2007). Indeed, ectopically expressed ZUFSP reacted with Ub-VS but not SUMO1-VS in a manner dependent on the predicted catalytic cysteine residue, C360 (Fig. 1C; Fig. S1B). Endogenous ZUFSP was also trapped by Ub-VS (Fig. 1D). Further supporting the notion that ZUFSP is a protease towards Ub but not UFM1, sequence alignment analysis revealed that the ZUFSP peptidase domain is more distantly related to the UFSP1/2 family than to the uncharacterized peptidase Mug105 in *S. pombe* (Fig. 1E), which does not express UFM1 (Komatsu et al., 2004). While *Sp*Mug105 lacks the N-terminal domain harboring the ZnF and MIU motifs found in ZUFSP (Fig. 1A), we found that, like ZUFSP, it reacted with Ub-VS in a manner dependent on its putative active site cysteine (C42) that aligns with C360 in human ZUFSP (Fig. 1B,F). Importantly, in contrast to ZUFSP and Mug105, human UFSP2 did not react with Ub-VS (Fig. S1C). Using purified recombinant ZUFSP, we detected clear protease activity of ZUFSP towards a minimal Ub-Rhodamine substrate that was fully abrogated by the C360A mutation (Fig. 1G). We conclude that ZUFSP has DUB activity by virtue of a C-terminal cysteine protease domain that is distinct from any known DUBs.

ZUFSP selectively interacts with long K63-linked Ub chains via tandem UBDs

Having shown that ZUFSP is a DUB, we next interrogated its Ub-binding capabilities. Using N- and C-terminally truncated ZUFSP fragments immunopurified from cells, we found that the Ub-binding determinant(s) localized to the N-terminal portion (Fig. 2A,B). In addition to the MIU, we noted that the ZnF motif in immediate proximity to the MIU, but not ZnFs1-3, strongly resembles a UBZ3 domain, a type of Ub-binding C2H2 ZnF that also resides in, and crucially promotes the function of, the translesion DNA synthesis (TLS) polymerase Polη (Fig. 2A,C) (Bienko et al., 2005; Hofmann, 2009). We surmised that this configuration might impart preferential binding of ZUFSP to Ub chains, as has been reported for other tandem UBDs (Husnjak and Dikic, 2012; Sims and Cohen, 2009). Indeed, we found that ZUFSP was highly selective for interaction with poly-Ub chains and bound recombinant mono-, di- and tri-Ub inefficiently *in vitro* (Fig. 2D). Importantly, the Ub-binding ability of ZUFSP was diminished by specific point mutations within the MIU or UBZ domains and nearly abrogated by simultaneous mutation of both motifs (Fig. 2E), suggesting they cooperatively underlie high-affinity ZUFSP binding to poly-Ub chains. Tandem configurations of UBDs can confer linkage-specific binding to Ub chains (Husnjak and Dikic, 2012; Sims and Cohen, 2009). Interestingly, using purified tetra-Ub linkages, we noted that ZUFSP displays a remarkable preference for interaction with K63-linked chains (Fig. 2F), suggesting that it may be involved in regulation of K63 ubiquitylation-mediated cellular processes. Varying the linker length between the UBZ and MIU motifs did not detectably affect the K63 chain-binding ability of ZUFSP (Fig. S1D), suggesting flexibility in the interdistance between these motifs.

ZUFSP selectively deubiquitylates K63 poly-Ub chains

We next probed the ability of ZUFSP to cleave different Ub linkages. In line with its preference for binding long Ub chains, we found that all eight di-Ub linkages were poor substrates of recombinant wild-type (WT) ZUFSP *in vitro* (Fig. S1E). When presented with longer Ub chains, however, ZUFSP displayed potent and selective DUB activity towards K63-linked chains while hydrolyzing other poly-Ub chains inefficiently (Fig. 3A-D; Fig. S1F). Consistent with its lack of activity against Ub-Rhodamine, the ZUFSP C360A mutant showed no detectable activity towards K63 chains (Fig. 1D; Fig. 3D). As tetra-K27 Ub chains were not available to us, we cannot rule out that in addition to K63-linked chains ZUFSP may also be able to cleave this linkage type, although it showed little activity towards K27 di-Ub linkages (Fig. S1E). Because the tandem UBZ/MIU motifs in ZUFSP confer selectivity for binding to K63-linked poly-Ub chains, which are also the preferred substrate of ZUFSP, we next asked whether the Ub-binding N-terminus was needed for ZUFSP activity towards these chains. Kinetic analysis of ZUFSP activity against Ub-Rhodamine revealed a 2-fold higher activity of full-length (FL) ZUFSP compared to the catalytic domain (CD) only (Fig. 3E). Detailed fitting of the data showed that the difference was in the K_M (K_M(FL)=4.9 μM; K_M(CD)=10.5 μM), while the rates (k_{cat}) were identical (k_{cat}=0.084 s^{-1}) (Fig. S2A-C), predicting cleavage of maximally 9% bonds per min in the first turnover under the conditions of Fig. 3D (1 μM enzyme, ~3 μM octa-Ub chains (~21 μM cleavable K63 linkages)), in good overall agreement with our findings. These kinetic constants also indicate that in comparison to a range of USP-type DUBs (Faesen et al., 2011), ZUFSP is a relatively slow enzyme towards minimal Ub substrates. Strikingly, when assayed for activity towards K63-linked poly-Ub chains, ZUFSP CD was virtually inactive, in contrast to ZUFSP FL (Fig. 3F). We conclude that ZUFSP selectively cleaves K63-linked poly-Ub chains in a manner that strictly

depends on its UBD-containing N-terminal portion, which may orient K63-linked chains for efficient hydrolysis by the peptidase domain.

K63-Ub-dependent recruitment of ZUFSP to genotoxic stress sites

As ZUFSP mainly localizes to the nucleus (Fig. 4A), contains MIU and UBZ domains and shows selectivity for binding to and processing K63-linked Ub chains, it shares several features with key DDR factors, and we therefore considered the possibility that ZUFSP functions in genome maintenance processes. Consistent with this idea, GFP-tagged ZUFSP was recruited to sites of localized DNA double-strand breaks (DSBs) induced by laser micro-irradiation or the FokI nuclease (Shanbhag and Greenberg, 2013) in a subset of cells (Fig. 4A,B; Fig. S3A). At the laser- and FokI-induced DSB sites, ZUFSP preferentially co-localized with RPA, which demarcates single-stranded DNA (ssDNA) regions generated in proximity to the breaks (Fig. S3A,B). Analysis of ZUFSP mutants revealed that both the UBDs and the three N-terminal ZnFs were required for ZUFSP accumulation at DNA damage sites (Fig. 2A; Fig. 4A,B). On the other hand, catalytically inactive ZUFSP formed foci in an increased proportion of cells, suggesting its potential trapping by one or more substrates at DNA damage sites (Fig. 4B). In line with the UBZ/MIU-mediated selective binding of ZUFSP to K63-linked Ub chains and the key role of this modification in promoting protein recruitment to DNA damage sites (Jackson and Durocher, 2013; Schwertman et al., 2016), knockdown of Ubc13, the major E2 Ub-conjugating enzyme responsible for K63 chain formation (Hofmann and Pickart, 1999) strongly impaired ZUFSP accumulation at DNA damage sites (Fig. 4C; Fig. S3C). Moreover, consistent with its enrichment at RPA-ssDNA regions at DSB sites, ZUFSP accumulation at FokI-induced DSBs was largely abrogated by knockdown of

CtIP, a critical mediator of DSB end-resection-generated ssDNA stretches (Fig. 4C; Fig. S3C) (Symington, 2014). However, despite ZUFSP associated with RPA in co-immunoprecipitation experiments, this interaction did not depend on its UBDs and ZnF motifs, and ZUFSP recruitment to DSBs was unaffected by RPA depletion (Fig. 4C; Fig. S3D), suggesting the involvement of additional factors and/or ssDNA binding *per se*.

ZUFSP catalytic activity promotes responses to replication stress

Extended ssDNA regions can form as a consequence of both DSB end-resection and replication stress (Symington, 2014; Zeman and Cimprich, 2014), raising the possibility that ZUFSP functions in these processes. While modulation of ZUFSP expression levels or functional status did not significantly impact end-resection, DSB repair efficiency and recruitment of key repair factors such as 53BP1 to DSB sites (Fig. S3E-H; data not shown), we uncovered a potential role for ZUFSP in promoting responses to replication stress. Specifically, loss of ZUFSP led to an elevated frequency of micronuclei in RPE-1 or U2OS cells subjected to replication stress induced by treatment with low doses of replication-perturbing agents including aphidicolin, hydroxyurea and camptothecin, indicative of an elevated level of chromosomal instability (Fig. 4D; Fig. S4A-D). Moreover, cells depleted of ZUFSP accrued more S phase-associated DNA damage and displayed an elevated proportion of DNA damage-containing (RPA foci-positive) micronuclei upon treatment with replication stress-inducing agents (Fig. 4E; Fig. S4E). This suggested that ZUFSP might facilitate DNA replication integrity during conditions of replication stress. In line with this, GFP-ZUFSP showed robust recruitment to a replication fork barrier induced by binding of LacR to an integrated *LacO* array at a single genomic locus

(Beuzer et al., 2014), with kinetics paralleling that of K63-Ub conjugates and PCNA (Fig. 4F; Fig. S4F). Knockdown of ZUFSP by independent siRNAs significantly increased K63-Ub levels at the LacR/*LacO* barrier (Fig. 4G), suggesting that ZUFSP regulates the K63 ubiquitylation status of one or more factors at replication stress sites. In addition, while loss of ZUFSP did not alter cell cycle distribution in unchallenged conditions, it markedly delayed cell cycle progression upon release from an HU-induced replication block, evidenced by a persistence of S phase cells at time points where the majority of control cells had completed DNA replication (Fig. 4H; Fig. S4G). Expression of WT ZUFSP fully rescued this delay (Fig. 4H). Finally, the increased incidence of replication stress-induced micronuclei caused by ZUFSP loss could be restored by complementation with stably expressed WT ZUFSP, whereas catalytically inactive and Ub-binding deficient mutants failed to correct this defect (Fig. 4I; Fig. S4H). Together, these findings suggest that ZUFSP has a role in preserving chromosomal stability after perturbations to normal DNA replication that requires both its K63 ubiquitylation-directed DUB activity and ability to interact with genotoxic stress sites.

Discussion

The findings reported here demonstrate that despite having been considered a potentially inactive UFM1 peptidase, ZUFSP harbors potent, linkage-selective DUB activity, displaying a marked preference for interacting with and cleaving long K63 poly-Ub chains. While the only other human protein that appears to contain a full ZUFSP-like peptidase domain is the UFM1-specific protease UFSP2, which we found has no detectable DUB activity, we note that this module is conserved through

eukaryotic evolution and that like human ZUFSP, the *S. pombe* orthologue Mug105 is also an active DUB. The ZUFSP/Mug105 family therefore appears to define a class of cysteine protease DUBs that is distinct from the five known thiol protease DUB families. Interestingly, ZUFSP has several features in common with MINDY-1, another recently identified human DUB whose biological function is unknown (Abdul Rehman et al., 2016). Accordingly, both of these factors show a clear preference for interacting with and cleaving long Ub chains and remarkable chain-trimming activity towards specific Ub linkages, mediated by tandem UBDs encompassing MIU motifs. However, in contrast to ZUFSP, MINDY-1 selectively recognizes and cleaves K48-linked poly-Ub chains (Abdul Rehman et al., 2016). Structural analysis of full-length ZUFSP will be important to fully address the molecular basis of its selectivity for recognizing and hydrolyzing K63-linked poly-Ub chains. While we cannot formally rule out that ZUFSP may also possess catalytic activity towards UFM1, we currently have no *in vitro* or *in vivo* evidence supporting this possibility. Based on our collective findings, we suggest renaming ZUFSP as ZUP1 (Zinc finger containing Ubiquitin Peptidase 1).

In line with the key role of K63-linked ubiquitylation in promoting the DDR (Jackson and Durocher, 2013; Schwertman et al., 2016), we uncovered an emerging function of ZUFSP DUB activity in maintaining chromosomal stability upon replication stress. Apart from the well-established role of K63-linked PCNA polyubiquitylation in promoting tolerance of DNA damage encountered during replication (Garcia-Rodriguez et al., 2016), detailed mechanistic insights into how non-proteolytic K63 ubiquitylation regulates responses to replication stress remain limited, and we have not obtained supportive evidence for a direct role of ZUFSP DUB activity in

reversing PCNA polyubiquitylation (data not shown). The selective activity of ZUFSP towards long K63-linked Ub chains suggests that it could function as a chain-trimming enzyme working in conjunction with other Ub signaling factors to ensure the proper dynamics of K63 ubiquitylation-dependent modifications of one or more proteins residing in the context of RPA-ssDNA regions at genotoxic stress sites. The potential complexity of such Ub-mediated regulatory processes is underscored by the extensive range of DUBs that have been implicated in genotoxic stress responses, often playing partially redundant roles (Kee and Huang, 2015). Precisely how ZUFSP DUB activity promotes these and possibly other biological responses will therefore be important yet challenging subjects of future investigations.

Acknowledgments

We thank Roger Greenberg and Susan Janicki for providing reagents and Alexander Fish (NKI Protein Facility) for assistance with kinetic modeling. This work was supported by grants from Novo Nordisk Foundation (grants no. NNF14CC0001 and NNF15OC0016926), European Research Council (ERC, grant agreement no. 616236 (DDRegulation)), Danish Council for Independent Research, The Lundbeck Foundation, Danish National Research Foundation (grant no. DNRF115), The Danish Cancer Society and The Dutch Cancer Society KWF (2015-8082). D.T. is a Marie Skłodowska-Curie Fellow (IF-Grant Number: 744866-ChroSoDSB).

Author contributions

Conceptualization, P.H. and N.M.; Methodology, P.H., N.B., X.G., D.T., D.A., S.H., R.S., T.S. and N.M. Investigation, P.H., N.B., X.G., D.T.; Writing – Original Draft, P.H. and N.M.; Writing – Review & Editing, P.H. and N.M.; Supervision, T.S. and N.M.; Project Administration, N.M.; Funding Acquisition, D.T., T.S. and N.M.

Declaration of Interests

The authors declare no competing interests.

References

Abdul Rehman, S.A., Kristariyanto, Y.A., Choi, S.Y., Nkosi, P.J., Weidlich, S., Labib, K., Hofmann, K., and Kulathu, Y. (2016). MINDY-1 Is a Member of an Evolutionarily Conserved and Structurally Distinct New Family of Deubiquitinating Enzymes. Mol Cell *63*, 146-155.

Beuzer, P., Quivy, J.P., and Almouzni, G. (2014). Establishment of a replication fork barrier following induction of DNA binding in mammalian cells. Cell Cycle *13*, 1607-1616.

Bienko, M., Green, C.M., Crosetto, N., Rudolf, F., Zapart, G., Coull, B., Kannouche, P., Wider, G., Peter, M., Lehmann, A.R., *et al.* (2005). Ubiquitin-binding domains in Y-family polymerases regulate translesion synthesis. Science *310*, 1821-1824.

Cai, Y., Pi, W., Sivaprakasam, S., Zhu, X., Zhang, M., Chen, J., Makala, L., Lu, C., Wu, J., Teng, Y., *et al.* (2015). UFBP1, a Key Component of the Ufm1 Conjugation System, Is Essential for Ufmylation-Mediated Regulation of Erythroid Development. PLoS Genet *11*, e1005643.

Chen, Z.J., and Sun, L.J. (2009). Nonproteolytic functions of ubiquitin in cell signaling. Mol Cell *33*, 275-286.

Cong, L., Ran, F.A., Cox, D., Lin, S., Barretto, R., Habib, N., Hsu, P.D., Wu, X., Jiang, W., Marraffini, L.A., *et al.* (2013). Multiplex genome engineering using CRISPR/Cas systems. Science *339*, 819-823.

Cope, G.A., Suh, G.S., Aravind, L., Schwarz, S.E., Zipursky, S.L., Koonin, E.V., and Deshaies, R.J. (2002). Role of predicted metalloprotease motif of Jab1/Csn5 in cleavage of Nedd8 from Cul1. Science *298*, 608-611.

Doil, C., Mailand, N., Bekker-Jensen, S., Menard, P., Larsen, D.H., Pepperkok, R., Ellenberg, J., Panier, S., Durocher, D., Bartek, J., *et al.* (2009). RNF168 binds and amplifies ubiquitin conjugates on damaged chromosomes to allow accumulation of repair proteins. Cell *136*, 435-446.

Elia, A.E., Boardman, A.P., Wang, D.C., Huttlin, E.L., Everley, R.A., Dephoure, N., Zhou, C., Koren, I., Gygi, S.P., and Elledge, S.J. (2015). Quantitative Proteomic Atlas

of Ubiquitination and Acetylation in the DNA Damage Response. Mol Cell *59*, 867-881.
Faesen, A.C., Luna-Vargas, M.P., Geurink, P.P., Clerici, M., Merkx, R., van Dijk, W.J., Hameed, D.S., El Oualid, F., Ovaa, H., and Sixma, T.K. (2011). The differential modulation of USP activity by internal regulatory domains, interactors and eight ubiquitin chain types. Chem Biol *18*, 1550-1561.
Garcia-Rodriguez, N., Wong, R.P., and Ulrich, H.D. (2016). Functions of Ubiquitin and SUMO in DNA Replication and Replication Stress. Front Genet *7*, 87.
Ha, B.H., Jeon, Y.J., Shin, S.C., Tatsumi, K., Komatsu, M., Tanaka, K., Watson, C.M., Wallis, G., Chung, C.H., and Kim, E.E. (2011). Structure of ubiquitin-fold modifier 1-specific protease UfSP2. J Biol Chem *286*, 10248-10257.
Hickey, C.M., Wilson, N.R., and Hochstrasser, M. (2012). Function and regulation of SUMO proteases. Nat Rev Mol Cell Biol *13*, 755-766.
Hochstrasser, M. (2009). Origin and function of ubiquitin-like proteins. Nature *458*, 422-429.
Hofmann, K. (2009). Ubiquitin-binding domains and their role in the DNA damage response. DNA Repair (Amst) *8*, 544-556.
Hofmann, R.M., and Pickart, C.M. (1999). Noncanonical MMS2-encoded ubiquitin-conjugating enzyme functions in assembly of novel polyubiquitin chains for DNA repair. Cell *96*, 645-653.
Husnjak, K., and Dikic, I. (2012). Ubiquitin-binding proteins: decoders of ubiquitin-mediated cellular functions. Annu Rev Biochem *81*, 291-322.
Jackson, S.P., and Durocher, D. (2013). Regulation of DNA damage responses by ubiquitin and SUMO. Mol Cell *49*, 795-807.
Janicki, S.M., Tsukamoto, T., Salghetti, S.E., Tansey, W.P., Sachidanandam, R., Prasanth, K.V., Ried, T., Shav-Tal, Y., Bertrand, E., Singer, R.H., *et al.* (2004). From silencing to gene expression: real-time analysis in single cells. Cell *116*, 683-698.
Johnson, K.A., Simpson, Z.B., and Blom, T. (2009a). FitSpace explorer: an algorithm to evaluate multidimensional parameter space in fitting kinetic data. Anal Biochem *387*, 30-41.
Johnson, K.A., Simpson, Z.B., and Blom, T. (2009b). Global kinetic explorer: a new computer program for dynamic simulation and fitting of kinetic data. Anal Biochem *387*, 20-29.
Kang, S.H., Kim, G.R., Seong, M., Baek, S.H., Seol, J.H., Bang, O.S., Ovaa, H., Tatsumi, K., Komatsu, M., Tanaka, K., *et al.* (2007). Two novel ubiquitin-fold modifier 1 (Ufm1)-specific proteases, UfSP1 and UfSP2. J Biol Chem *282*, 5256-5262.
Kee, Y., and Huang, T.T. (2015). Role of Deubiquitinating Enzymes in DNA Repair. Mol Cell Biol *36*, 524-544.
Kim, W., Bennett, E.J., Huttlin, E.L., Guo, A., Li, J., Possemato, A., Sowa, M.E., Rad, R., Rush, J., Comb, M.J., *et al.* (2011). Systematic and quantitative assessment of the ubiquitin-modified proteome. Mol Cell *44*, 325-340.
Komander, D., and Rape, M. (2012). The ubiquitin code. Annu Rev Biochem *81*, 203-229.
Komatsu, M., Chiba, T., Tatsumi, K., Iemura, S., Tanida, I., Okazaki, N., Ueno, T., Kominami, E., Natsume, T., and Tanaka, K. (2004). A novel protein-conjugating system for Ufm1, a ubiquitin-fold modifier. EMBO J *23*, 1977-1986.
Kulathu, Y., and Komander, D. (2012). Atypical ubiquitylation - the unexplored world of polyubiquitin beyond Lys48 and Lys63 linkages. Nat Rev Mol Cell Biol *13*, 508-523.

Lee, S., Tsai, Y.C., Mattera, R., Smith, W.J., Kostelansky, M.S., Weissman, A.M., Bonifacino, J.S., and Hurley, J.H. (2006). Structural basis for ubiquitin recognition and autoubiquitination by Rabex-5. Nat Struct Mol Biol *13*, 264-271.
Luna-Vargas, M.P., Christodoulou, E., Alfieri, A., van Dijk, W.J., Stadnik, M., Hibbert, R.G., Sahtoe, D.D., Clerici, M., Marco, V.D., Littler, D., *et al.* (2011). Enabling high-throughput ligation-independent cloning and protein expression for the family of ubiquitin specific proteases. J Struct Biol *175*, 113-119.
Malakhov, M.P., Malakhova, O.A., Kim, K.I., Ritchie, K.J., and Zhang, D.E. (2002). UBP43 (USP18) specifically removes ISG15 from conjugated proteins. J Biol Chem *277*, 9976-9981.
Mevissen, T.E.T., and Komander, D. (2017). Mechanisms of Deubiquitinase Specificity and Regulation. Annu Rev Biochem *86*, 159-192.
Mosbech, A., Gibbs-Seymour, I., Kagias, K., Thorslund, T., Beli, P., Povlsen, L., Nielsen, S.V., Smedegaard, S., Sedgwick, G., Lukas, C., *et al.* (2012). DVC1 (C1orf124) is a DNA damage-targeting p97 adaptor that promotes ubiquitin-dependent responses to replication blocks. Nat Struct Mol Biol *19*, 1084-1092.
Nijman, S.M., Luna-Vargas, M.P., Velds, A., Brummelkamp, T.R., Dirac, A.M., Sixma, T.K., and Bernards, R. (2005). A genomic and functional inventory of deubiquitinating enzymes. Cell *123*, 773-786.
Ovaa, H. (2007). Active-site directed probes to report enzymatic action in the ubiquitin proteasome system. Nat Rev Cancer *7*, 613-620.
Panier, S., Ichijima, Y., Fradet-Turcotte, A., Leung, C.C., Kaustov, L., Arrowsmith, C.H., and Durocher, D. (2012). Tandem protein interaction modules organize the ubiquitin-dependent response to DNA double-strand breaks. Mol Cell *47*, 383-395.
Penengo, L., Mapelli, M., Murachelli, A.G., Confalonieri, S., Magri, L., Musacchio, A., Di Fiore, P.P., Polo, S., and Schneider, T.R. (2006). Crystal structure of the ubiquitin binding domains of rabex-5 reveals two modes of interaction with ubiquitin. Cell *124*, 1183-1195.
Poulsen, M., Lukas, C., Lukas, J., Bekker-Jensen, S., and Mailand, N. (2012). Human RNF169 is a negative regulator of the ubiquitin-dependent response to DNA double-strand breaks. J Cell Biol *197*, 189-199.
Schwertman, P., Bekker-Jensen, S., and Mailand, N. (2016). Regulation of DNA double-strand break repair by ubiquitin and ubiquitin-like modifiers. Nat Rev Mol Cell Biol *17*, 379-394.
Shanbhag, N.M., and Greenberg, R.A. (2013). The dynamics of DNA damage repair and transcription. Methods Mol Biol *1042*, 227-235.
Sims, J.J., and Cohen, R.E. (2009). Linkage-specific avidity defines the lysine 63-linked polyubiquitin-binding preference of rap80. Mol Cell *33*, 775-783.
Stewart, G.S., Panier, S., Townsend, K., Al-Hakim, A.K., Kolas, N.K., Miller, E.S., Nakada, S., Ylanko, J., Olivarius, S., Mendez, M., *et al.* (2009). The RIDDLE syndrome protein mediates a ubiquitin-dependent signaling cascade at sites of DNA damage. Cell *136*, 420-434.
Symington, L.S. (2014). End resection at double-strand breaks: mechanism and regulation. Cold Spring Harbor perspectives in biology *6*, a016436.
Tang, J., Cho, N.W., Cui, G., Manion, E.M., Shanbhag, N.M., Botuyan, M.V., Mer, G., and Greenberg, R.A. (2013). Acetylation limits 53BP1 association with damaged chromatin to promote homologous recombination. Nat Struct Mol Biol *20*, 317-325.
Tatsumi, K., Sou, Y.S., Tada, N., Nakamura, E., Iemura, S., Natsume, T., Kang, S.H., Chung, C.H., Kasahara, M., Kominami, E., *et al.* (2010). A novel type of E3 ligase for the Ufm1 conjugation system. J Biol Chem *285*, 5417-5427.

Tatsumi, K., Yamamoto-Mukai, H., Shimizu, R., Waguri, S., Sou, Y.S., Sakamoto, A., Taya, C., Shitara, H., Hara, T., Chung, C.H., *et al.* (2011). The Ufm1-activating enzyme Uba5 is indispensable for erythroid differentiation in mice. Nat Commun *2*, 181.
Tkac, J., Xu, G., Adhikary, H., Young, J.T., Gallo, D., Escribano-Diaz, C., Krietsch, J., Orthwein, A., Munro, M., Sol, W., *et al.* (2016). HELB Is a Feedback Inhibitor of DNA End Resection. Mol Cell *61*, 405-418.
Toledo, L.I., Altmeyer, M., Rask, M.B., Lukas, C., Larsen, D.H., Povlsen, L.K., Bekker-Jensen, S., Mailand, N., Bartek, J., and Lukas, J. (2013). ATR prohibits replication catastrophe by preventing global exhaustion of RPA. Cell *155*, 1088-1103.
van der Veen, A.G., and Ploegh, H.L. (2012). Ubiquitin-like proteins. Annu Rev Biochem *81*, 323-357.
Wagner, S.A., Beli, P., Weinert, B.T., Nielsen, M.L., Cox, J., Mann, M., and Choudhary, C. (2011). A proteome-wide, quantitative survey of in vivo ubiquitylation sites reveals widespread regulatory roles. Mol Cell Proteomics *10*, M111 013284.
Wu, X., and Karin, M. (2015). Emerging roles of Lys63-linked polyubiquitylation in immune responses. Immunol Rev *266*, 161-174.
Zeman, M.K., and Cimprich, K.A. (2014). Causes and consequences of replication stress. Nat Cell Biol *16*, 2-9.

Figure legends

Figure 1.

ZUFSP is a deubiquitylating enzyme

A. Domain organization of human (*Hs*) ZUFSP and *Schizosaccharomyces pombe* (*Sp*) Mug105, showing location of predicted N-terminal ZnF, UBZ and MIU motifs and a C-terminal C78 Papain-like peptidase domain. **B**. Alignment of predicted ZUFSP catalytic cysteine and histidine residues based on the structure of UFSP2 (Ha et al., 2011). Asterisk (*) marks the catalytic cysteine (C360) in ZUFSP. **C**. Extracts of U2OS cell lines stably expressing GFP-ZUFSP WT or C360A mutant were incubated with HA-tagged Ub-VS and subjected to HA immunoprecipitation (IP) followed by immunoblotting with indicated antibodies. Asterisk (*) indicates non-specific binding of GFP-ZUFSP to HA agarose. **D**. As in (C), but using extracts of U2OS cells or a derivative *ZUFSP* knockout (*ZUFSP*Δ) line. **E**. Average distance tree based on

alignment of the C78 peptidase domains and PAM250 scoring of the indicated proteins, showing that ZUFSP is more closely related to Mug105 than UFSP1/2. **F**. As in (C), using U2OS cells transfected with plasmids encoding GFP-Mug105 WT or C42A mutant. Asterisk (*) indicates non-specific binding of GFP-Mug105 to HA agarose. **G**. *In vitro* activity of recombinant ZUFSP WT and C360A towards Ub-Rhodamine.

See also Fig. S1.

Figure 2.

ZUFSP interacts with long K63-linked Ub chains via tandem UBZ and MIU motifs

A. Schematic of ZUFSP fragments used in (B) and (E). **B**. GFP-ZUFSP proteins expressed in HEK293 cells were immunopurified on GFP-Trap agarose, incubated with recombinant K63-Ub_{3-7} chains and washed extensively. Bound complexes were immunoblotted with Ub antibody. **C**. Alignment of MIU motifs in ZUFSP and other human proteins (left), and of the ZUFSP UBZ domain with UBZ3 domains in human and *Drosophila melanogaster* (*Dm*) Polymerase η (Polη). **D**. As in (B), using GFP-ZUFSP WT and recombinant mono-Ub or indicated K63-Ub chains. **E**. Binding of GFP-ZUFSP alleles containing inactivating point mutations in the UBZ and MIU motifs to Ub-$K63_{1-7}$ chains was analyzed as in (B). **F**. Analysis of GFP-ZUFSP WT binding to indicated tetra-K63 chains was performed as in (B).

See also Fig. S1.

Figure 3.

ZUFSP selectively deubiquitylates K63 poly-Ub chains

A. Purified recombinant ZUFSP WT was incubated with indicated tetra-Ub linkages for 0 or 4 h. Reactions were resolved by SDS-PAGE and visualized by silver staining. **B**. Quantification of ZUFSP activity towards different tetra-Ub linkages (A). Ratios between tetra-Ub levels at 4 h and 0 h were determined by ImageJ Gel Analysis (mean±SEM; *n*=3 independent experiments). **C**. As in (A), but using K48- or K63-linked penta-Ub chains. **D**. Time-course analysis of ZUFSP WT and C360A activity towards K63-Ub_8 chains, performed as in (A). **E**. Michaelis-Menten analysis of ZUFSP full-length (FL) and catalytic domain only (CD) (50 nM enzyme). Initial rates were taken at 15 s. **F**. Activity of full-length ZUFSP or CD towards K63-Ub_8 chains was analyzed as in (A).

See also Fig. S1, S2.

Figure 4.

ZUFSP promotes responses to replication stress

A. U2OS/ER-mCherry-LacR-FokI-DD/*LacO* cells (Tang et al., 2013) transfected with empty vector expressing GFP only or GFP-ZUFSP constructs were treated with 4-hydroxytamoxifen and Shield-1 for 5 h to induce clustered DSBs in a single *LacO* genomic locus (white arrow), then fixed and immunostained with γ-H2AX antibody. Representative images are shown. Scale bar, 10 μm. **B**. Quantification of results from (A), showing proportion of GFP-positive cells with GFP accumulation at FokI/γH2AX foci (mean±SEM; at least 100 cells quantified per condition per experiment; *n*=3-7 independent experiments; ****p<0.0001, ***p<0.0005, unpaired t-test with Welch's correction). **C**. U2OS/ER-mCherry-LacR-FokI-DD/*LacO* cells were transfected with indicated siRNAs, then transfected with GFP-ZUFSP WT plasmid and processed for DSB induction and immunostaining as in (A). Proportion

of GFP-positive cells with GFP accumulation at FokI/γH2AX foci was determined (mean±SEM normalized to siCTRL; 15-45 cells quantified per condition per experiment; *n*=3 independent experiments; **p<0.005, unpaired t-test with Welch's correction). See also Fig. S3C. **D**. hTERT-RPE-1 cells transfected with indicated siRNAs were treated for 24 h with 0.2 μM aphidicolin (APH), 10 nM camptothecin (CPT) or 0.2 mM hydroxyurea (HU) prior to fixation and DAPI staining. Proportion of cells with micronuclei was determined (mean±SEM; 400-800 cells quantified per condition per experiment; *n*=5 independent experiments; *p<0.05, **p<0.005, n.s. not significant, unpaired t-test with Welch's correction). **E**. U2OS and derivative cells stably expressing GFP-ZUFSP WT were transfected with 3' UTR-targeting ZUFSP siRNA (siZUFSP#20), treated with CPT for 1 h, washed and released into fresh medium for 24 h prior to fixation and immunostaining with RPA2 antibody in the presence of DAPI. Proportion of RPA2-positive micronuclei (example marked by arrow) was scored (mean±SEM; 50-70 micronuclei analyzed per condition per experiment; *n*=2-4 independent experiments). **F**. Representative images of U2OS/2-6-3 cells carrying a single *LacO* array (white arrow) that were synchronized at the G1/S border by a double thymidine block, transfected with constructs encoding GFP-ZUFSP or GFP empty vector (EV), then released into S phase for 2 or 6 h in the presence of LacR-mCherry expression and fixed and immunostained with PCNA antibody. In the lower panel, cells were additionally pre-extracted and co-immunostained with K63-Ub antibody. Scale bar, 10 μm. See Fig. S4F for additional time points. **G**. As in (F, lower panel), except that cells were transfected with indicated siRNAs. K63-Ub signal at individual LacR/*LacO* arrays (corrected for nuclear background signal) was quantified in cells released 6 h into S phase (bars, mean; >100 arrays analyzed per condition per experiment; ****p<0.0001, Mann-

Whitney test). Data from a representative experiment are shown. **H**. U2OS and U2OS/GFP-ZUFSP cell lines transfected with control (CTRL) or 3' UTR-targeting ZUFSP siRNA (siZUFSP#20) were treated with HU (2 mM) for 12 h, and where indicated washed and released into fresh medium for an additional 12 h. Cells were then immunostained with PCNA antibody in the presence of DAPI. Cell cycle profiles were determined by quantification of total DAPI content per nucleus. PCNA chromatin loading was used to determine the proportion of S phase cells (indicated). Data from a representative experiment are shown. **I**. As in (D), but using U2OS cells or derivative lines stably expressing GFP-ZUFSP transgenes (Fig. S4H) transfected with control (−) or a ZUFSP siRNA targeting the 3'-UTR (+) and treated with 0.2 μM aphidicolin for 24 h (mean±SEM; 300-800 cells quantified per condition per experiment; *n*=3 independent experiments; *p<0.05, **p<0.005, n.s. not significant, unpaired t-test with Welch's correction).

See also Fig. S3,S4.

STAR Methods

KEY RESOURCES TABLE

Provided as a separate file uploaded along with this submission.

CONTACT FOR REAGENT AND RESOURCE SHARING

Further information and requests for resources and reagents should be directed to and will be fulfilled by the Lead Contact, Niels Mailand (niels.mailand@cpr.ku.dk).

EXPERIMENTAL MODEL AND SUBJECT DETAILS

Source of cell lines used in the study is reported in the Key Resources Table.

METHOD DETAILS

Plasmids and siRNAs

Full-length human *ZUFSP* and *UFSP2* cDNAs (in pENTR221 entry vector) were obtained from the Invitrogen Ultimate™ ORF Collection. Human codon-optimized *mug105* cDNA was produced as a synthetic gene (IDT Gene Synthesis). Point mutations and deletions in ZUFSP (C360A; MIU*: A237G; UBZ*: C195G,C198G; ΔZnF1-3: deletion of amino acids (aa) 2-177; ΔCD: deletion of aa335-578; and Δ1-310: deletion of aa1-310; Linker(+3): insertion of AAA after Q222; Linker(Δ3): deletion of aa 223-225) and Mug105 PD* (C42A) were introduced with the Q5 Site-directed Mutagenesis Kit (NEB), according to the manufacturer's protocol. Using Gateway LR Clonase (Invitrogen), cDNAs were inserted into the destination vector pcDNA4/TO/EGFP for doxycycline-inducible expression. For bacterial expression, cDNA encoding full-length human ZUFSP or the catalytic domain (CD) only (aa315-578) was inserted into pGEX-6P-1 (Sigma Aldrich), or pET-NKI-his3C-LIC vector using ligation-independent cloning (Luna-Vargas et al., 2011). Plasmids for generation of U2OS *ΔZUFSP* cells using CRISPR/Cas9 were generated as described (Cong et al., 2013) using the pX459 plasmid (Addgene #62988) for Cas9 and gRNA delivery. Briefly, gRNA sequences were ordered as complementary primers, mixed in a 1:1 ratio and annealed. Subsequently, pX459 was digested with BbsI and the gRNA introduced using a normal ligation reaction according to the manufacturer's instructions (New England Biolabs). The following sequences were used: ZUFSP sgRNA #3 (forward): 5'-CACCGGCGACAAAGGTTGGGGTTG-3'; ZUFSP sgRNA #3 (reverse): 5'-AAACCAACCCCAACCTTTGTCGCC-3'; ZUFSP sgRNA #14

(forward): 5’-CACCGAGCTCACCTAATTGTTCACA-3’; ZUFSP sgRNA #14 (reverse): 5’-AAACTGTGAACAATTAGGTGAGCTC-3’. U2OS/*ZUFSPΔ* clones #1 and #2 were derived from ZUFSP sgRNA #3, and U2OS/*ZUFSPΔ* #3 from ZUFSP sgRNA #14.

Plasmid DNA and siRNA transfections were performed using FuGENE 6 Transfection Reagent (Promega) and Lipofectamine RNAiMAX (Invitrogen), respectively, according to the manufacturers’ protocols. All siRNAs were used at a final concentration of 50 nM unless otherwise indicated. The following siRNA oligonucleotides were used: Non-targeting control (CTRL): 5’-GGGAUACCUAGACGUUCUA-3’; ZUFSP(#9): 5’-GCAGAGACAAUAUGGUUUA -3’; ZUFSP(#20) (targeting the 3’UTR): 5’-CUAAAAUGCCUGUGUUAAU-3’; RAD51: 5’-GUAGAGAAGUGGAGCGUAA-3’; Ubc13: 5’-GAGCAUGGACUAGGCUAUA-3'; RPA1: 5’-GGAAUUAUGUCGUAAGUCA-3'; CtIP: 5’-GCUAAAACAGGAACGAAUC-3’.

Cell culture

Human U2OS, HEK293 and hTERT-RPE-1 cells were obtained from ATCC. All cell lines used in this study were cultured in DMEM containing 10% FBS, and were regularly tested for mycoplasma infection. The cell lines were not authenticated. To generate U2OS cell lines inducibly expressing GFP-ZUFSP WT and mutant alleles, U2OS cells were co-transfected with pcDNA4/TO/GFP-ZUFSP constructs and pcDNA6/TR (Invitrogen) and positive clones were selected by incubation in medium containing blasticidin S (Invitrogen) and zeocin (Invitrogen) for 14 days. To generate U2OS *ZUFSPΔ* cell lines, parental cells were transfected with pX459-sgZUFSP #3 or #14 (gRNAs targeting unique sequences within the *ZUFSP* locus) and selected briefly

with puromycin during clonal selection. Clones were screened for ZUFSP expression by immunoblotting.

Unless otherwise indicated, the following drug concentrations were used: camptothecin (10 nM, Sigma Aldrich), hydroxyurea (0.2 mM, Sigma Aldrich), aphidicolin (0.2 μM, Sigma Aldrich), and doxycycline (1 μg/ml, Sigma Aldrich).

Immunoblotting, cell fractionation and antibodies

For immunoblotting and immunoprecipitation, which were done as described (Poulsen et al., 2012), cells were lysed in EBC buffer (50 mM Tris, pH 7.5; 150 mM NaCl; 1 mM EDTA; 0.5% NP40; 1 mM DTT) supplemented with protease and phosphatase inhibitors. Lysates were then incubated 10 min on ice and sonicated. For immunoprecipitations, lysates were additionally treated with benzonase to minimize chromatin-mediated interactions.

Antibodies used in this study included: 53BP1 (sc-22760, Santa Cruz (1:500)), Actin (MAB1501, Millipore (1:20,000 dilution), CHK1 pSer345 (2348, Cell Signaling (1:1,000)), CHK2 pThr68 (2661, Cell Signaling (1:500)), CtIP (A300-488A, Bethyl (1:1,000)), GFP (sc-9996 (Clone B2), Santa Cruz (1:1,000)), γ-H2AX (05-636 (Clone JBW301), Millipore (1:500)), HA (11867423001 (Clone 3F10), Roche (1:1,000)), p97 (ab11433, Abcam (1:5,000)), RAD51 (PC130, Ab-1, Millipore (1:500)), RPA1 (Ab79398, Abcam (1:1,000)), RPA2 (NA19L (Clone Ab-3), Calbiochem (1:1,000)), RPA2 pSer4/Ser8 (A300-245A, Bethyl (1:1,000)), PCNA (#2037, Triolab Immunoconcepts (1:500)), Polyubiquitin K63 linkage-specific (BML-PW0600, Enzo life sciences (1:200)), SENP6 (NPB1-82958, Novus Bio (1:5,000)), Ubc13 (37-1100 (Clone 4E11), Invitrogen (1:3,000)), Ubiquitin (sc-8017 (Clone P4D1), Santa Cruz (1:1,000)), USP7 (A300-033A, Bethyl (1:5,000)). Polyclonal sheep antibody to

ZUFSP was raised against full-length recombinant human ZUFSP, purified from bacteria.

Purification of recombinant ZUFSP proteins

GST-ZUFSP, GST-ZUFSP C360A and His_6-ZUFSP CD were expressed in *E. coli* RosettaTM2(DE3) induced with 0.2 mM IPTG and grown at 20 °C overnight. For GST-ZUFSP and GST-ZUFSP C360A, cells were pelleted and resuspended in 50 mM HEPES pH 7.5; 150 mM NaCl; 1 mM DTT and Pierce protease inhibitor. Cells were lysed on ice by sonication (Qsonica) in the presence of 5 µg/ml DNase I (Sigma). The cell lysate was centrifuged at 30,000g for 40 min at 4 °C. The supernatant was first clarified by a 0.45-µm-syringe filter and loaded onto a gravity column containing 3 ml Glutathione Sepharose 4B (GE Healthcare) and incubated at 4 °C for 30 min. The resin was washed with 20 mM HEPES pH 7.5; 600 mM NaCl; 1 mM DTT, and then eluted with 20 mM HEPES, pH 7.5; 150 mM NaCl; 1mM DTT; 20mM glutathione. The GST-tag was removed by 3C protease at 4 °C for 4 h. Finally, the tag-free protein was loaded onto the Hiload 16/60 Superdex 200 column equilibrated in 20 mM HEPES pH 7.5; 150 mM NaCl; 1 mM DTT. The elution fractions containing ZUFSP or ZUFSP C360A were concentrated to desired concentration. His_6-ZUFSP CD was purified in a similar way as GST-ZUFSP, but lysed in 50 mM Tris-HCl, pH 8.0; 200 mM NaCl; 20 mM imidazole; 1 mM DTT and Pierce protease inhibitor. The supernatant from centrifugation was loaded onto 2 ml Ni-Sepharose columns and washed with 50 mM Tris-HCl, pH 8.0; 200 mM NaCl; 20 mM imidazole; 1 mM DTT. The protein was eluted by 50 mM Tris-HCl, pH 8.0; 200 mM NaCl; 500 mM imidazole; 1mM DTT, and further purified by a Hiload 16/60 Superdex 75 column equilibrated with 20 mM HEPES; 200 mM NaCl; 1 mM DTT.

DUB assays

To assay for reactivity of peptidases with Ub- and SUMO vinyl sulfone (VS) probes, U2OS cells were lysed under mild conditions (50 mM Tris, pH 8.0; 50mM NaCl; 5mM DTT; 0.2% Triton X-100; 50 µM PMSF), briefly sonicated and cleared by centrifugation. The lysate was then incubated with 0.5 µM recombinant HA-tagged Ub-VS or SUMO1-VS (#U-212-025 and # UL-703-050, Boston Biochem) for 1 h at 37°C with gentle shaking, diluted in denaturing buffer (20 mM Tris, pH 7.5; 50 mM NaCl; 1 mM EDTA; 1 mM DTT; 0.5% NP-40; 0.5% sodium deoxycholate; 0.5% SDS) and subjected to immunoprecipitation with anti-HA agarose (A2095, Sigma Aldrich) followed by immunoblotting.

For analysis of ZUFSP activity towards purified Ub chains (purchased from Boston Biochem and pre-diluted to 0.3 µg/µL in 2xDUB buffer (100 mM NaCl, 100 mM Tris-HCl, pH 7.5; 10 mM DTT)), recombinant ZUFSP was diluted to 2 µM in DUB dilution buffer (150 mM NaCl; 25mM Tris-HCl, pH 7.5; 10 mM DTT), incubated at room temperature for 15 min, mixed 1:1 with Ub chains and incubated at 30 °C with gentle shaking. Reactions were terminated by addition of Laemmli sample buffer and boiled for 5 min. Samples were resolved by SDS-PAGE and analyzed by silver staining (Pierce Silver Stain Kit, Thermo Scientific) according to the manufacturer's instructions.

Enzyme activity against Ub N-terminal Rhodamine (Boston Biochem) was measured by a Pherastar fluorescence plate reader (BMG) with 384-well non-binding surface, flat bottom, low flange, black plates (Corning). The fluorescence intensity from free Rhodamine was detected using 480 nm as excitation and 520 nm as emission wavelengths. All enzymes and substrate were prepared in 20 mM HEPES, pH7.5; 150 mM NaCl; 1 mM DTT; 0.02% Tween-20; 1 mg/ml BSA, and all experiments were done at 25 °C. For single-point assays 100 nM ZUFSP WT or C360A were injected

into wells containing 15 µl Ub-Rhodamine (1 µM) in a total volume of 30 µl. For kinetic analysis of ZUFSP FL and CD, a plate was prepared with serially diluted 30 µM Ub-Rhodamine (15 µl fractions), and the reaction was started by injection of 15 µl enzyme within the Pherastar. Fluorescence signals were recorded from 1.5 s after injection, at 1-s intervals until 50.5 s. Each enzyme was analyzed at 3 different concentrations (200 nM, 100 nM and 50 nM) and all measurements were repeated twice. For analysis, we performed detailed kinetic analysis and kinetic modeling using the software KinTek Explorer 6.3 (Johnson et al., 2009a, b). In this analysis we used a simple Michaelis-Menten model with correction for the signal decrease due to the adsorption of free Rhodamine to well surfaces. The association constant was fixed (k_{on}=10 $\mu M^{-1}s^{-1}$) to reflect a diffusion-limited process.

Ub-binding assays

HEK293 or U2OS cells expressing GFP-ZUFSP alleles were lysed in denaturing buffer supplemented with protease inhibitors, and extracts were sonicated and cleared by centrifugation. GFP-tagged ZUFSP was then purified on GFP-Trap agarose (Chromotek) followed by extensive washing in denaturing buffer. The beads were equilibrated in EBC buffer and incubated with recombinant Ub chains (0.5-1 µg/sample, Boston Biochem) for 2 h at 4°C with rotation. Bound material was washed 5 times in EBC buffer, eluted by boiling in 2x Laemmli sample buffer for 5 min and analyzed by immunoblotting. Pull-down experiments with Ub, SUMO1, SUMO2 and UFM1 coupled to agarose beads via primary amines (Boston Biochem) were performed using similar binding buffer (EBC) and washing conditions.

Immunofluorescence and high-content imaging analysis

Cells were pre-extracted in PBS containing 0.2% Triton X-100 for 2 min on ice, before fixation with 4% formaldehyde for 10 min. If cells were not pre-extracted, they

were subjected a permeabilization step with PBS containing 0.2% Triton X-100 for 5 min and incubated with primary antibodies diluted in 1% BSA-PBS for 1 h at room temperature. Following staining with secondary antibodies (Alexa Fluor; Life Technologies) diluted in 1% BSA-PBS for 1 h at room temperature, coverslips were mounted in Vectashield mounting medium (Vector Laboratories) containing nuclear stain DAPI. Laser microirradiation was performed as described (Mosbech et al., 2012). Induction and analysis of FokI-induced DSBs was done as described previously (Tang et al., 2013). Briefly, U2OS 2-6-5 cells expressing inducible ER-mCherry-LacR-FokI-DD (a kind gift from Roger Greenberg, University of Pennsylvania) were treated with 4-hydroxytamoxifen (300 nM, Sigma Aldrich) and Shield-I (1 µM, Clontech) for 5 h to allow for the expression of and induction of DSBs by the FokI nuclease. Cells were then fixed, permeabilized and immunostained as described. Analysis of LacR-induced replication blockage in U2OS 2-6-3 cells carrying a single *LacO* array on Chromosome 1 (a kind gift from Susan Janicki, University of Pennsylvania) (Janicki et al., 2004) was performed by synchronizing cells at the G1/S border by a double thymidine block. Cells were then washed extensively and released into S phase while expressing LacR-mCherry. Subsequently, cells were fixed, permeabilized and immunostained at regular intervals (2, 4, 6, 10 h) to establish the replication timing of the array (PCNA) and recruitment kinetics of GFP-ZUFSP and endogenous K63-linked poly-Ub (cells were pre-extracted to detect K63-linked poly-Ub).

Images were acquired with a Leica AF6000 wide-field microscope (Leica Microsystems) equipped with HC Plan-Apochromat 63x/1.4 oil immersion objective, using standard settings. Image acquisition and analysis was carried out with LAS X software (Leica Microsystems). Raw images were exported as TIFF files and if

adjustments in image contrast and brightness were applied, identical settings were used on all images of a given experiment. For cell cycle analysis by EdU staining, cells were treated with EdU (10 μM) for 30 min before fixation, then stained using the Click-iT® Plus EdU Alexa Fluor 647 Imaging Kit (Invitrogen) according to the manufacturer's instructions. Quantitative image-based cytometry (QIBC) was performed as described (Toledo et al., 2013). Briefly, cells were fixed, permeabilised and stained as described above. Nuclear DNA was counterstained with DAPI (Molecular Probes) alongside incubation with secondary antibodies. Cells were mounted onto glass slides using ProLong® Gold Antifade (Invitrogen, Molecular Probes). Images were acquired with an Olympus IX-81 wide-field microscope equipped with an MT20 Illumination system and a digital monochrome Hamamatsu C9100 CCD camera. Olympus UPLSAPO 10x/0.4 NA, 20x/0.75 NA objectives were used. Automated and unbiased image analysis was carried out with the ScanR analysis software. Data was exported and processed using Spotfire (Tibco) software.

QUANTIFICATION AND STATISTICAL ANALYSIS

Statistical analysis of data was performed using GraphPad Prism (version 7). Information about statistical tests is provided in the figure legends. No samples were excluded from the analysis and no statistical method was used to predetermine sample size. For all experiments, samples were not randomized and the investigators were not blinded to the group allocation during experiments and outcome assessment.

DATA AND SOFTWARE AVAILABILITY

Original imaging data have been deposited to Mendeley Data and are available at http://dx.doi.org/10.17632/89twmd4sd7.1.

CellPress

TABLE FOR AUTHOR TO COMPLETE

Please upload the completed table as a separate document. ***Please do not add subheadings to the Key Resources Table.*** *If you wish to make an entry that does not fall into one of the subheadings below, please contact your handling editor. (****NOTE:*** *For authors publishing in Current Biology, please note that references within the KRT should be in numbered style, rather than Harvard.)*

KEY RESOURCES TABLE

REAGENT or RESOURCE	SOURCE	IDENTIFIER
Antibodies		
anti-53BP1	Santa Cruz Biotechnology	Cat# sc-22760
Anti-Actin	Millipore	Cat# MAB1501
Anti-CHK1 pSer345	Cell Signaling	Cat# 2348
Anti-CHK2 pThr68	Cell Signaling	Cat# 2661
Anti-CtIP	Bethyl	Cat# A300-488A
Anti-GFP	Santa Cruz Biotechnology	Cat# sc-9996
Anti-γ-H2AX	Millipore	Cat# 05-636
Anti-HA-tag	Roche	Cat# 11867423001
Anti-p97	Abcam	Cat# Ab11433
Anti-RAD51	Millipore	Cat# PC130
anti-RPA1	Abcam	Cat# Ab79398
Anti-RPA2	Calbiochem	Cat# NA19L
Anti-RPA2 pSer4/Ser8	Bethyl	Cat# A300-245A
Anti-PCNA	Triolab Immunoconcepts	Cat# 2037
Anti-SENP6	Novus Bio	Cat# NPB1-82958
Anti-Ubc13	Invitrogen	Cat# 37-1100
Anti-Ubiquitin	Santa Cruz Biotechnology	Cat# sc-8017
Anti-USP7	Bethyl	Cat# A300-033A
Anti-K63-Ub	Enzo life sciences	Cat# BML-PW0600
Sheep polyclonal Anti-ZUFSP	Custom made	N/A
Anti-mouse 488	Molecular probes	Cat# A-11001
Anti-human 647	TriChem	Cat# 709-606-149
Anti-rabbit 488	Molecular probes	Cat# A-11008
Anti-mouse 568	Molecular probes	Cat# A-10037
Anti-rabbit 568	Molecular probes	Cat# A-11011
Anti-mouse HRP	Vector laboratories	Cat# PI-2000
Anti-rabbit HRP	Vector laboratories	Cat# PI-1000
Anti-sheep HRP	DAKO	Cat# P0163
Bacterial and Virus Strains		
E. coli RosettaTM2(DE3)	N/A	N/A

Chemicals, Peptides, and Recombinant Proteins		
Camptothecin	Sigma Aldrich	Cat# C9911
Hydroxyurea	Sigma Aldrich	Cat# H8627
Aphidicolin	Sigma Aldrich	Cat# A0781
Doxycycline	Sigma Aldrich	Cat# D9891
4-hydroxytamoxifen	Sigma Aldrich	Cat# H7904
Shield-I	Clontech	Cat# 632188
Thymidine	Sigma Aldrich	Cat# T9250
Protein inhibitor cocktail	Sigma Aldrich	Cat# P2714
Phosphatase inhibitor cocktail	Roche	Cat# 04906837001
Benzonase	Sigma Aldrich	Cat# E1014
Blasticidin S	Invitrogen	Cat# ant-bl-1
Zeocin	Gibco	Cat# R25005
FuGENE 6 Transfection Reagent	Promega	Cat# E2692
Lipofectamine RNAiMAX	Invitrogen	Cat# 13778150
DAPI	Molecular Probes	Cat# D1306
ProLong Gold Antifade	Molecular Probes	Cat# P36930
GFP-Trap agarose	Chromotek	Cat# gta-100
IPTG	AppliChem	Cat# A4773
Ubiquitin agarose	Boston Biochem	Cat# U-400
UFM1 agarose	Boston Biochem	Cat# UL-530
SUMO1 agarose	Boston Biochem	Cat# UL-740
SUMO2 agarose	Boston Biochem	Cat# UL-755
HA-Ubiquitin-VS	Boston Biochem	Cat# U-212-025
HA-SUMO1-VS	Boston Biochem	Cat# UL-703-050
Anti-HA agarose	Sigma Aldrich	Cat# A2095
Ub-Rhodamine110	Boston Biochem	Cat# U-555
Ub_2, M1-linked	Boston Biochem	Cat# UC-700B
Ub_2, K6-linked	Boston Biochem	Cat# UC-11B
Ub_2, K11-linked	Boston Biochem	Cat# UC-40B
Ub_2, K27-linked	Boston Biochem	Cat# UC-61
Ub_2, K29-linked	Boston Biochem	Cat# UC-81B
Ub_2, K33-linked	Boston Biochem	Cat# UC101B
Ub_2, K48-linked	Boston Biochem	Cat# UC-200B
Ub_2, K63-linked	Boston Biochem	Cat# UC-300B
Ub_4, M1-linked	Boston Biochem	Cat# UC-710B
Ub_4, K6-linked	Boston Biochem	Cat# UC-15
Ub_4, K11-linked	Boston Biochem	Cat# UC-45
Ub_4, K29-linked	Boston Biochem	Cat# UC-83
Ub_4, K33-linked	Boston Biochem	Cat# UC-103
Ub_4, K48-linked	Boston Biochem	Cat# UC-210B
Ub_4, K63-linked	Boston Biochem	Cat# UC-310B
Ub_5, K48-linked	Boston Biochem	Cat# UC-216
Ub_5, K63-linked	Boston Biochem	Cat# UC-316

Ub_8, K63-linked	Boston Biochem	Cat# UC-318
Ub_{1-7}, K63-linked	Boston Biochem	Cat# UC-340
Ub_{3-7}, K63-linked	Boston Biochem	Cat# UC-320
Recombinant ZUFSP (FL)	This paper	N/A
Recombinant ZUFSP (CD)	This paper	N/A
Recombinant ZUFSP C360A	This paper	N/A
Critical Commercial Assays		
Pierce Silver Stain Kit	Thermo Scientific	Cat# 24612
Click-iT Plus EdU Alexa Fluor 647 Imaging Kit	Invitrogen	Cat# C10640
Q5 Site-directed Mutagenesis Kit	NEB	Cat# E0554S
Deposited Data		
Raw imaging data	This paper	http://dx.doi.org/10.17632/89twmd4sd7.1
Experimental Models: Cell Lines		
U2OS	ATCC	HTB-96
HEK293T	ATCC	CRL-11268
hTERT-RPE-1	ATCC	CRL-4000
U2OS GFP-ZUFSP WT	This paper	N/A
U2OS GFP-ZUFSP C360A	This paper	N/A
U2OS GFP-ZUFSP MIU* (A237G)	This paper	N/A
U2OS GFP-ZUFSP UBZ* (C195G/C198G)	This paper	N/A
U2OS GFP-ZUFSP MIU* + UBZ*	This paper	N/A
U2OS GFP-ZUFSP ΔZnF1-3 (ΔAA2-177)	This paper	N/A
U2OS *ZUFSPΔ*	This paper	N/A
U2OS 2-6-3	Susan Janicki lab	Janicki et al., 2004
U2OS 2-6-5 ER-mCherry-lacR-FokI-DD	Roger Greenberg lab	Tang et al., 2013
Experimental Models: Organisms/Strains		
Oligonucleotides		
siCTRL: 5'-GGGAUACCUAGACGUUCUA-3'	Thorslund et al., 2015	N/A
siZUFSP(#9): 5'-GCAGAGACAAUAUGGUUUA -3'	This paper	N/A
siZUFSP(#20): 5'-CUAAAAUGCCUGUGUUAAU-3'	This paper	N/A
siRAD51: 5'-GUAGAGAAGUGGAGCGUAA-3'	Haahr et al., 2016	N/A
siUbc13: 5'-GAGCAUGGACUAGGCUAUA-3'	Thorslund et al., 2015	N/A
siRPA1: 5'-GGAAUUAUGUCGUAAGUCA-3'	Haahr et al., 2016	N/A
siCtIP: 5'-GCUAAAACAGGAACGAAUC-3'	Haahr et al., 2016	N/A
ZUFSP sgRNA#3 (forward): 5'-CACCGGCGACAAAGGTTGGGGTTG-3'	This paper	N/A
ZUFSP sgRNA#3 (reverse): 5'-AAACCAACCCCAACCTTTGTCGCC-3'	This paper	N/A
ZUFSP sgRNA#14 (forward): 5'-CACCGAGCTCACCTAATTGTTCACA-3'	This paper	N/A

ZUFSP sgRNA#14 (reverse): 5'-AAACTGTGAACAATTAGGTGAGCTC-3'	This paper	N/A
Recombinant DNA		
pcDNA4/TO/EGFP	Invitrogen	
pcDNA4/TO/EGFP ZUFSP WT	This paper	N/A
pcDNA4/TO/EGFP ZUFSP C360A	This paper	N/A
pcDNA4/TO/EGFP ZUFSP MIU*	This paper	N/A
pcDNA4/TO/EGFP ZUFSP UBZ*	This paper	N/A
pcDNA4/TO/EGFP ZUFSP MIU* + UBZ*	This paper	N/A
pcDNA4/TO/EGFP ZUFSP ΔZnF1-3	This paper	N/A
pcDNA4/TO/EGFP ZUFSP Δ1-310	This paper	N/A
pcDNA4/TO/EGFP ZUFSP ΔCD	This paper	N/A
pcDNA4/TO/EGFP ZUFSP Linker+3	This paper	N/A
pcDNA4/TO/EGFP ZUFSP LinkerΔ3	This paper	N/A
pcDNA4/TO/EGFP UFSP2	This paper	N/A
pcDNA4/TO/EGFP Mug105	This paper	N/A
pcDNA4/TO/EGFP Mug105 C42A	This paper	N/A
pGEX-6P-1	Sigma Aldrich	
pGEX-6P-1 ZUFSP FL	This paper	N/A
pGEX-6P-1 ZUFSP CD (AA315-578)	This paper	N/A
pET-NKI-his3C-LIC	Titia Sixma lab	N/A
pET-NKI-his3C-LIC ZUFSP FL	This paper	N/A
pET-NKI-his3C-LIC ZUFSP CD	This paper	N/A
pX459	Feng Zhang lab	Addgene plasmid #48139
pX459-ZUFSP sgRNA#3	This paper	N/A
pX459-ZUFSP sgRNA#14	This paper	N/A
Software and Algorithms		
GraphPad Prism 7 for Mac OS X	GraphPad Software	https://www.graphpad.com/scientific-software/prism/
ImageJ	ImageJ Software	https://imagej.net/Downloads
ScanR analysis software	Olympus	https://www.olympus-lifescience.com/
Spotfire software	Tibco	https://spotfire.tibco.com/
LAS X Software	Leica Microsystems	https://www.leica-microsystems.com
KinTek Explorer, Version 6.3	KinTek Corporation	https://kintekcorp.com/software/
Other		

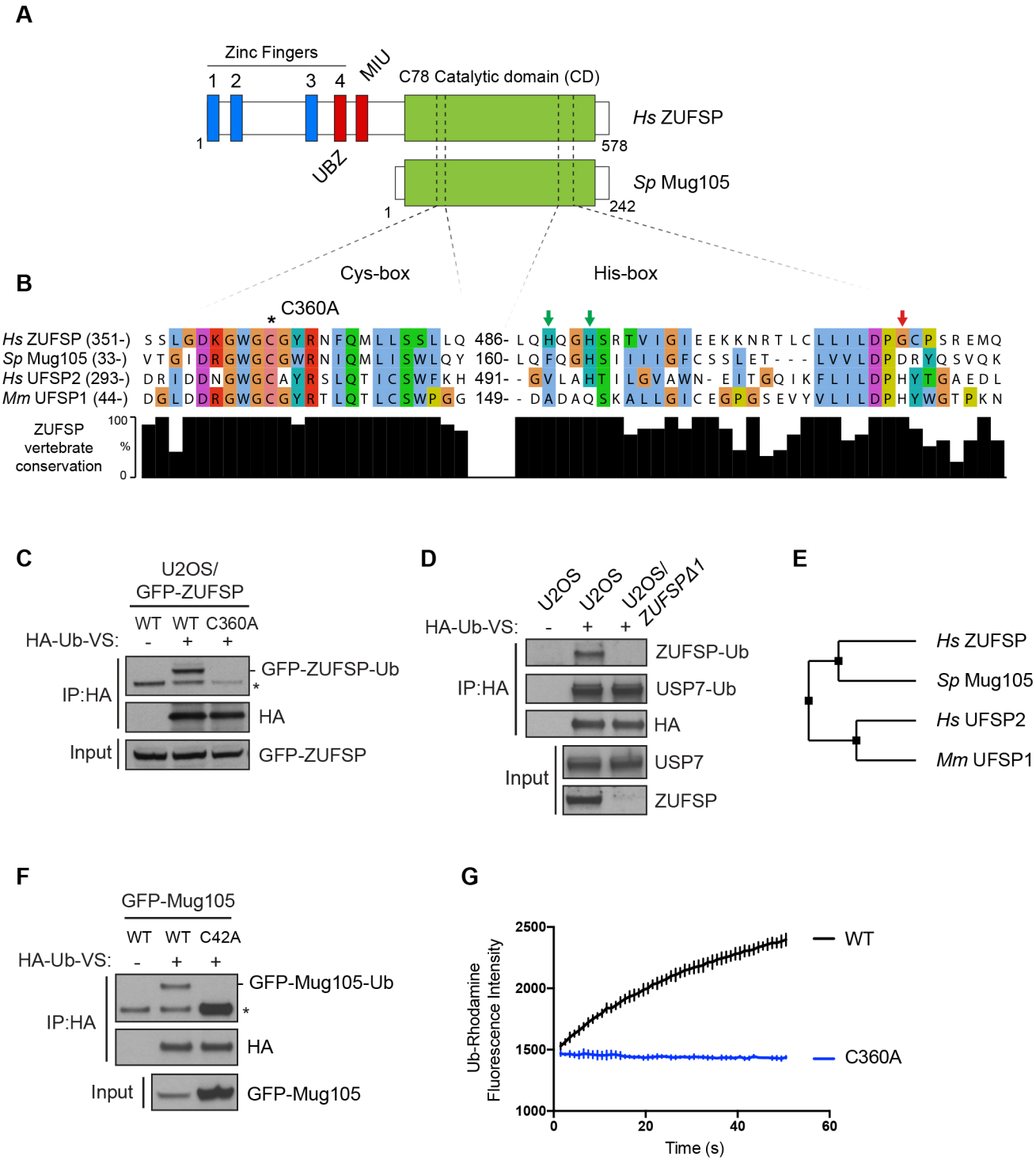
A
Zinc Fingers
1 2
3 4
MIU
C78 Catalytic domain (CD)
Hs ZUFSP
1
578
UBZ
Sp Mug105
1
242
B
Cys-box
His-box
C360A
Hs ZUFSP (351-) S S L G D K G W G C G Y R N F Q M L L S S L L Q 486- L Q H Q G H S R T V I G I E E K K N R T L C L L I L D P G C P S R E M Q
Sp Mug105 (33-) V T G I D R G W G C G W R N I Q M L I S W L Q Y 160- L Q F Q G H S I I I I G F C S S L E T - - - L V V L D P D R Y Q S V Q K
Hs UFSP2 (293-) D R I D D N G W G C A Y R S L Q T I C S W F K H 491- - G V L A H T I L G V A W N - E I T G Q I K F L I L D P H Y T G A E D L
Mm UFSP1 (44-) D G L D D R G W G C G Y R T L Q T L C S W P G G 149- - D A D A Q S K A L L G I C E G P G S E V Y V L I L D P H Y W G T P K N
ZUFSP vertebrate conservation
100
%
0
C
U2OS/ GFP-ZUFSP
WT WT C360A
HA-Ub-VS: - + +
IP:HA
GFP-ZUFSP-Ub
*
HA
Input
GFP-ZUFSP
D
U2OS
U2OS
U2OS/ ZUFSPΔ1
HA-Ub-VS: - + +
IP:HA
ZUFSP-Ub
USP7-Ub
HA
Input
USP7
ZUFSP
E
Hs ZUFSP
Sp Mug105
Hs UFSP2
Mm UFSP1
F
GFP-Mug105
WT WT C42A
HA-Ub-VS: - + +
IP:HA
GFP-Mug105-Ub
*
HA
Input
GFP-Mug105
G
Ub-Rhodamine Fluorescence Intensity
2500
2000
1500
1000
0
20
40
60
Time (s)
WT
C360A

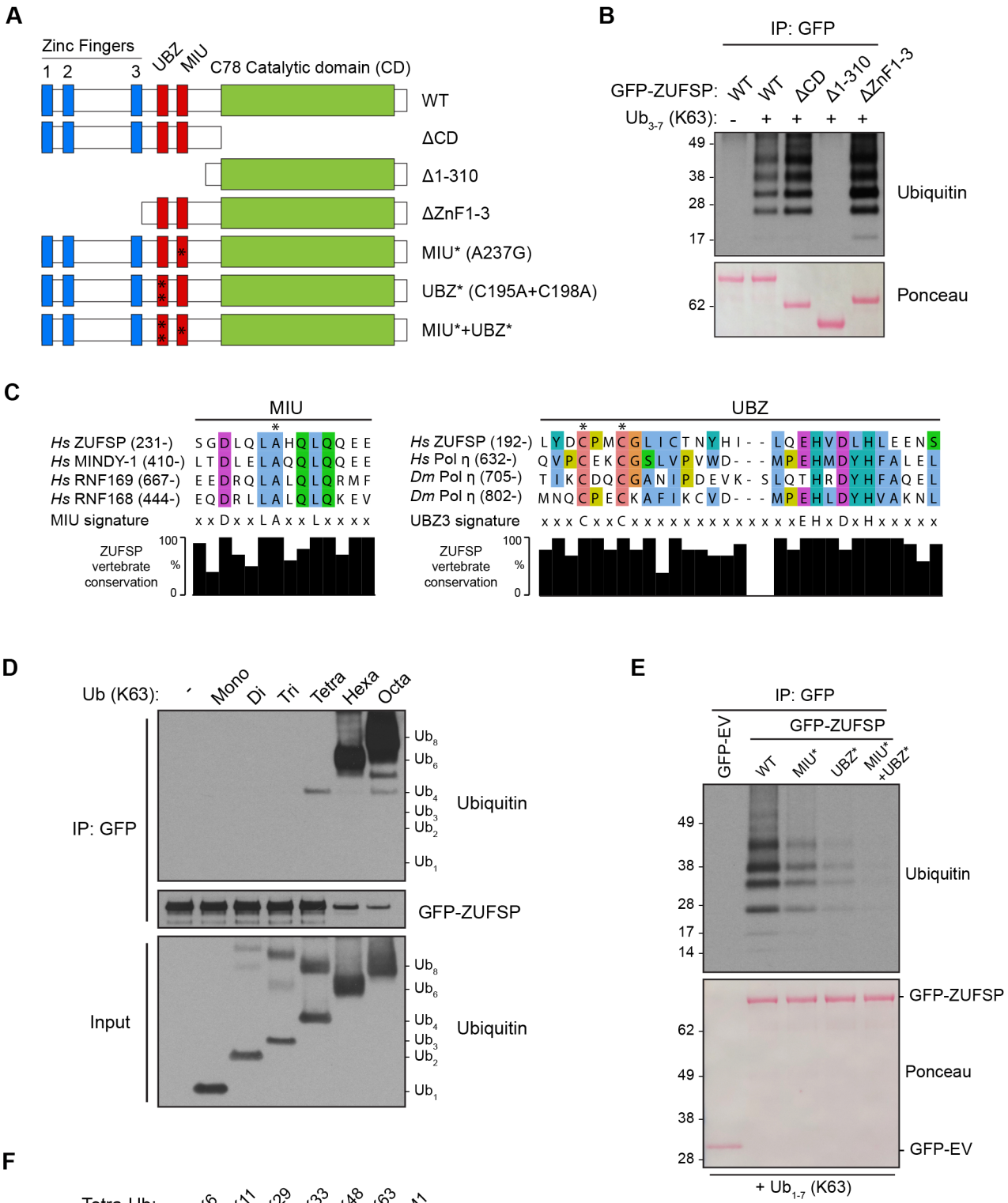
A
Zinc Fingers
1 2 3
UBZ
MIU
C78 Catalytic domain (CD)
WT
ΔCD
Δ1-310
ΔZnF1-3
MIU* (A237G)
UBZ* (C195A+C198A)
MIU*+UBZ*
B
IP: GFP
GFP-ZUFSP: WT WT ΔCD Δ1-310 ΔZnF1-3
Ub3-7 (K63): - + + + +
49
38
28
17
62
Ubiquitin
Ponceau
C
MIU
UBZ
Hs ZUFSP (231-) S G D L Q L A H Q L Q Q E E
Hs MINDY-1 (410-) L T D L E L A Q Q L Q Q E E
Hs RNF169 (667-) E E D R Q L A L Q L Q R M F
Hs RNF168 (444-) E Q D R L L A L Q L Q K E V
MIU signature x x D x x L A x x L x x x x
Hs ZUFSP (192-) L Y D C P M C G L I C T N Y H I - - L Q E H V D L H L E E N S
Hs Pol η (632-) Q V P C E K C G S L V P V W D - - M P E H M D Y H F A L E L
Dm Pol η (705-) T I K C D Q C G A N I P D E V K - S L Q T H R D Y H F A Q E L
Dm Pol η (802-) M N Q C P E C K A F I K C V D - - M P E H L D Y H V A K N L
UBZ3 signature x x x C x x C x x x x x x x x x x x x x E H x D x H x x x x x
ZUFSP vertebrate conservation
100
%
0
D
Ub (K63): - Mono Di Tri Tetra Hexa Octa
IP: GFP
Ub8
Ub6
Ub4
Ub3
Ub2
Ub1
Ubiquitin
GFP-ZUFSP
Input
Ubiquitin
E
IP: GFP
GFP-EV
GFP-ZUFSP
WT MIU* UBZ* MIU* +UBZ*
49
38
28
17
14
62
Ubiquitin
GFP-ZUFSP
Ponceau
GFP-EV
+ Ub1-7 (K63)
F
Tetra-Ub: - K6 K11 K29 K33 K48 K63 M1
IP: GFP-ZUFSP
28
Ubiquitin
GFP-ZUFSP (Ponceau)
Input (Ub)
28
Ubiquitin

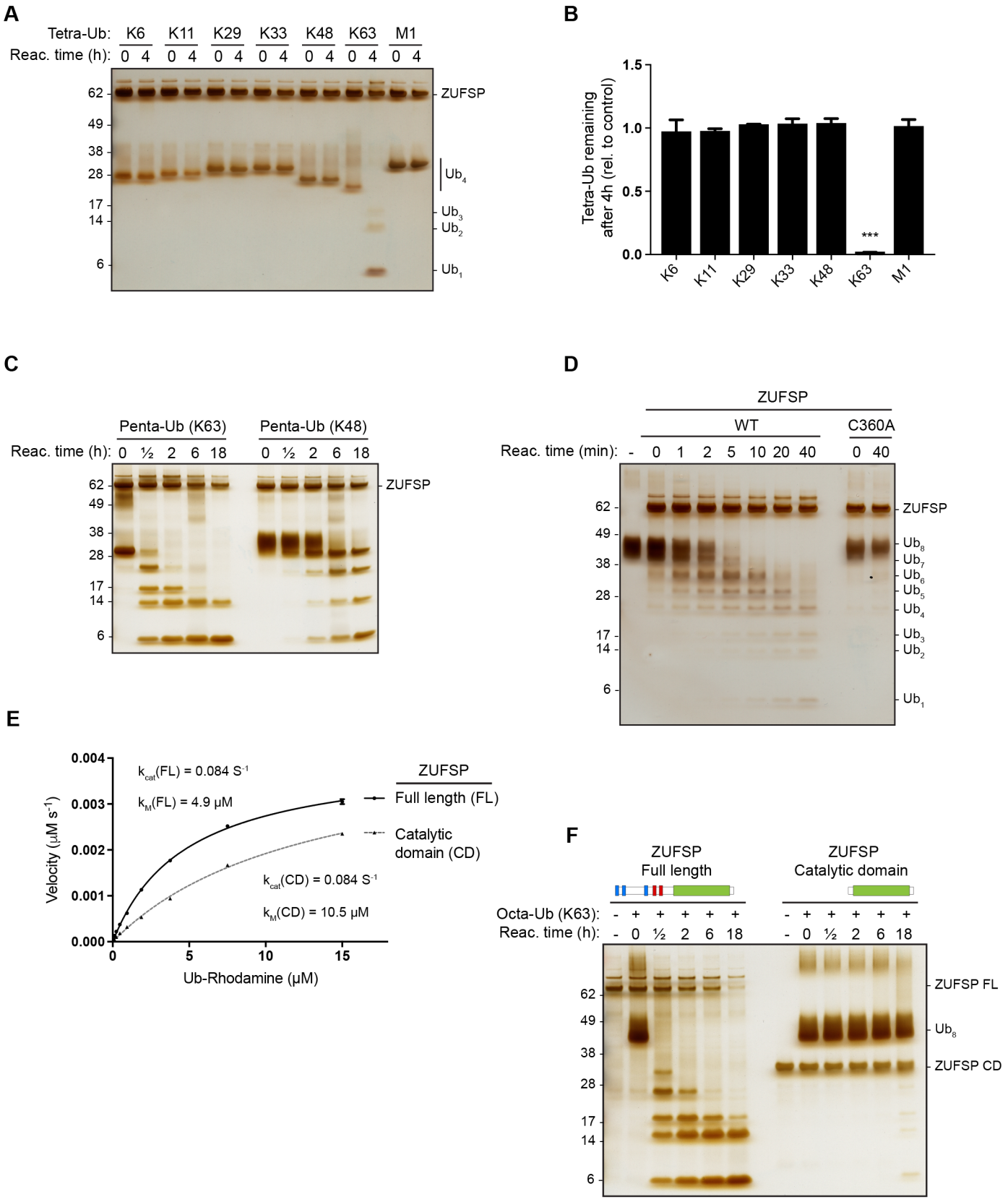
A
Tetra-Ub: K6 K11 K29 K33 K48 K63 M1
Reac. time (h): 0 4 0 4 0 4 0 4 0 4 0 4 0 4
62
49
38
28
17
14
6
ZUFSP
Ub4
Ub3
Ub2
Ub1
B
Tetra-Ub remaining after 4h (rel. to control)
1.5
1.0
0.5
0.0
***
K6
K11
K29
K33
K48
K63
M1
C
Penta-Ub (K63)
Penta-Ub (K48)
Reac. time (h): 0 ½ 2 6 18 0 ½ 2 6 18
62
49
38
28
17
14
6
ZUFSP
D
ZUFSP
WT
C360A
Reac. time (min): - 0 1 2 5 10 20 40 0 40
62
49
38
28
17
14
6
ZUFSP
Ub8
Ub7
Ub6
Ub5
Ub4
Ub3
Ub2
Ub1
E
Velocity (μM s-1)
0.004
0.003
0.002
0.001
0.000
0
5
10
15
Ub-Rhodamine (μM)
kcat(FL) = 0.084 S-1
kM(FL) = 4.9 μM
kcat(CD) = 0.084 S-1
kM(CD) = 10.5 μM
ZUFSP
Full length (FL)
Catalytic domain (CD)
F
ZUFSP Full length
ZUFSP Catalytic domain
Octa-Ub (K63): - + + + + + - + + + + +
Reac. time (h): - 0 ½ 2 6 18 - 0 ½ 2 6 18
62
49
38
28
17
14
6
ZUFSP FL
Ub8
ZUFSP CD

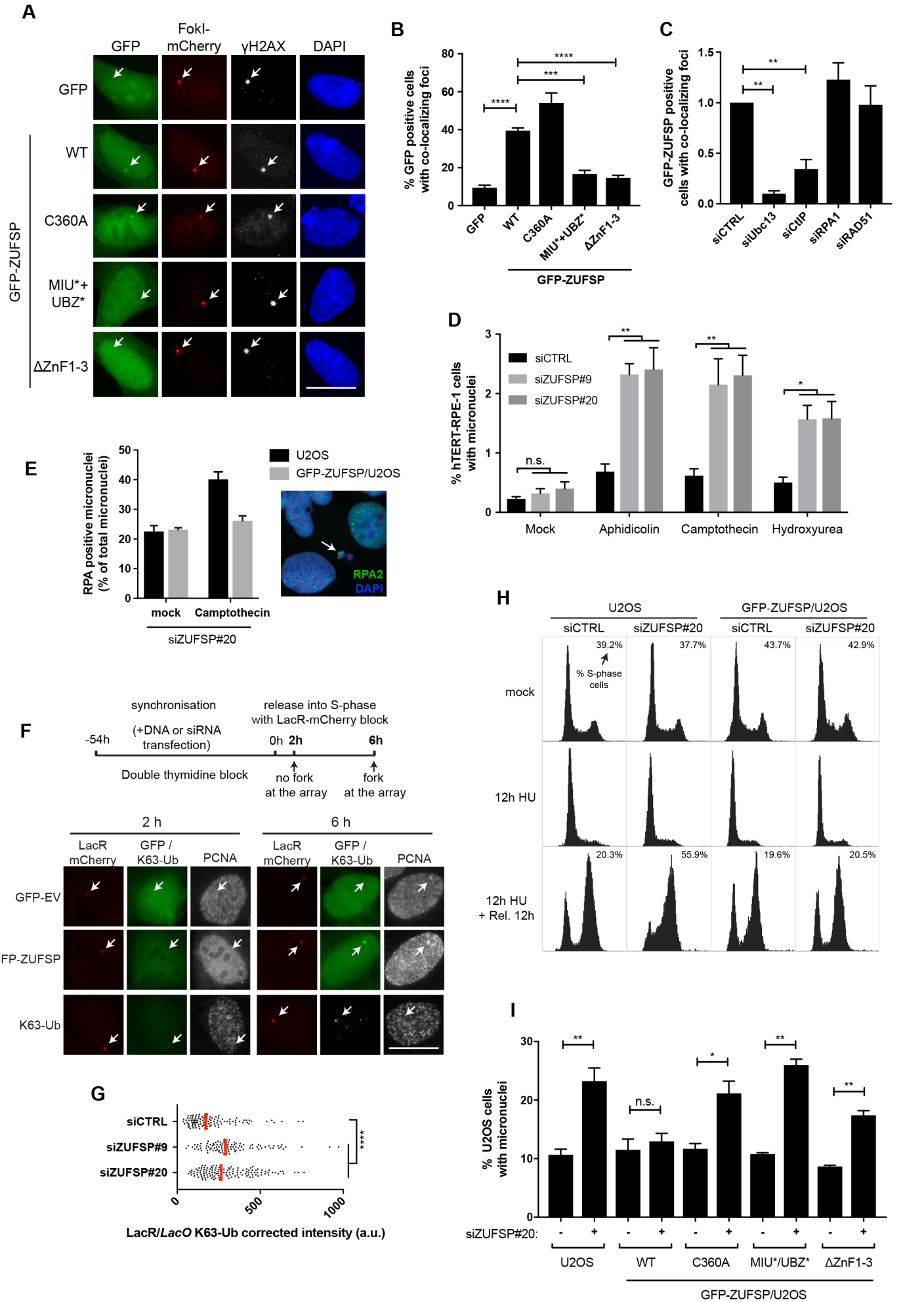
A
GFP
FokI-mCherry
γH2AX
DAPI
GFP
WT
C360A
MIU*+ UBZ*
ΔZnF1-3
GFP-ZUFSP
B
% GFP positive cells with co-localizing foci
GFP
WT
C360A
MIU*+UBZ*
ΔZnF1-3
GFP-ZUFSP
C
GFP-ZUFSP positive cells with co-localizing foci
siCTRL
siUbc13
siCtIP
siRPA1
siRAD51
D
% hTERT-RPE-1 cells with micronuclei
siCTRL
siZUFSP#9
siZUFSP#20
n.s.
Mock
Aphidicolin
Camptothecin
Hydroxyurea
E
RPA positive micronuclei (% of total micronuclei)
U2OS
GFP-ZUFSP/U2OS
RPA2
DAPI
mock
Camptothecin
siZUFSP#20
F
synchronisation
(+DNA or siRNA transfection)
release into S-phase with LacR-mCherry block
-54h
0h
2h
6h
Double thymidine block
no fork at the array
fork at the array
2 h
6 h
LacR mCherry
GFP / K63-Ub
PCNA
GFP-EV
GFP-ZUFSP
K63-Ub
G
siCTRL
siZUFSP#9
siZUFSP#20
LacR/LacO K63-Ub corrected intensity (a.u.)
H
U2OS
GFP-ZUFSP/U2OS
siCTRL
siZUFSP#20
% S-phase cells
39.2%
37.7%
43.7%
42.9%
mock
12h HU
20.3%
55.9%
19.6%
20.5%
12h HU + Rel. 12h
I
% U2OS cells with micronuclei
n.s.
siZUFSP#20:
U2OS
WT
C360A
MIU*/UBZ*
ΔZnF1-3
GFP-ZUFSP/U2OS

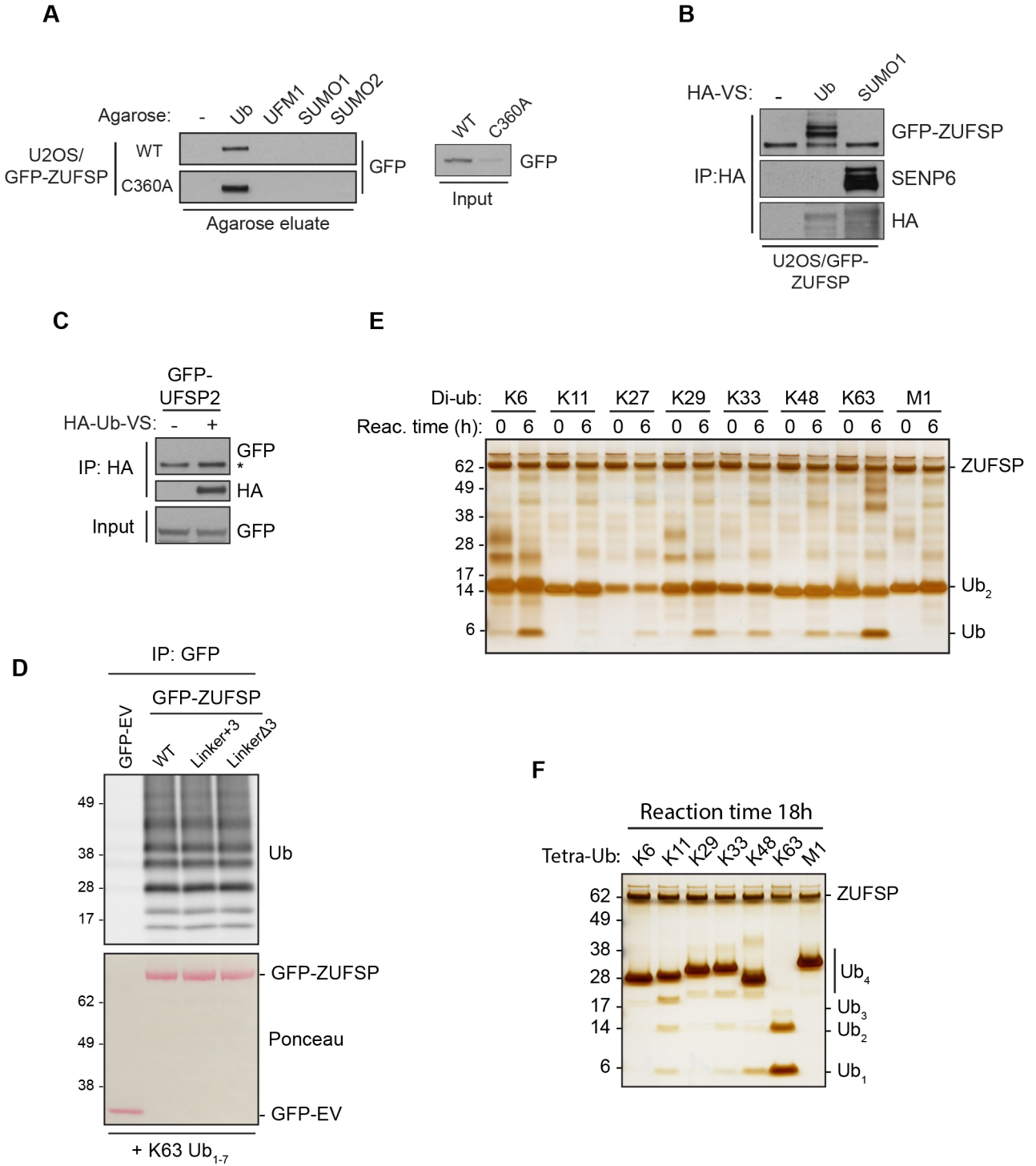
A
Agarose:
-
Ub
UFM1
SUMO1
SUMO2
U2OS/
GFP-ZUFSP
WT
C360A
GFP
Agarose eluate
WT
C360A
GFP
Input
B
HA-VS:
-
Ub
SUMO1
GFP-ZUFSP
IP:HA
SENP6
HA
U2OS/GFP-
ZUFSP
C
GFP-
UFSP2
HA-Ub-VS:
-
+
IP: HA
GFP
*
HA
Input
GFP
D
IP: GFP
GFP-ZUFSP
GFP-EV
WT
Linker+3
LinkerΔ3
49
38
28
17
Ub
62
49
38
GFP-ZUFSP
Ponceau
GFP-EV
+ K63 Ub1-7
E
Di-ub:
K6
K11
K27
K29
K33
K48
K63
M1
Reac. time (h):
0 6 0 6 0 6 0 6 0 6 0 6 0 6 0 6
62
49
38
28
17
14
6
ZUFSP
Ub2
Ub
F
Reaction time 18h
Tetra-Ub:
K6
K11
K29
K33
K48
K63
M1
62
49
38
28
17
14
6
ZUFSP
Ub4
Ub3
Ub2
Ub1

Figure S1. Related to Figure 1-3

Ub-binding and DUB activity of ZUFSP

A. Extracts of U2OS cells stably expressing indicated GFP-ZUFSP alleles were incubated with immobilized Ub, UFM1-, SUMO1- or SUMO2-agarose, washed extensively and immunoblotted with GFP antibody. **B**. Extracts of U2OS cells stably expressing GFP-ZUFSP WT were incubated with HA-tagged Ub or SUMO1 vinyl sulfone (VS), subjected to HA immunoprecipitation followed by immunoblotting with indicated antibodies. SENP6 is a positive control for reactivity with SUMO1-VS. **C**. Extracts of U2OS cells transiently transfected with GFP-UFSP2 expression plasmid were treated as in (B). **D**. GFP-only (empty vector, EV) or GFP-ZUFSP proteins containing a three-amino acid insertion (Linker+3) or deletion (LinkerΔ3) were expressed in HEK293 cells and immunopurified on GFP-Trap agarose, incubated with recombinant K63-Ub_{1-7} chains and washed extensively. Bound complexes were immunoblotted with Ub antibody. **E**. Bacterially purified, recombinant ZUFSP WT was incubated with indicated di-Ub linkages for 0 or 6 h. Reactions were resolved by SDS-PAGE and visualized by silver staining. **F**. As in (E), except that recombinant ZUFSP WT was incubated with indicated tetra-Ub linkages for 18 h.

A

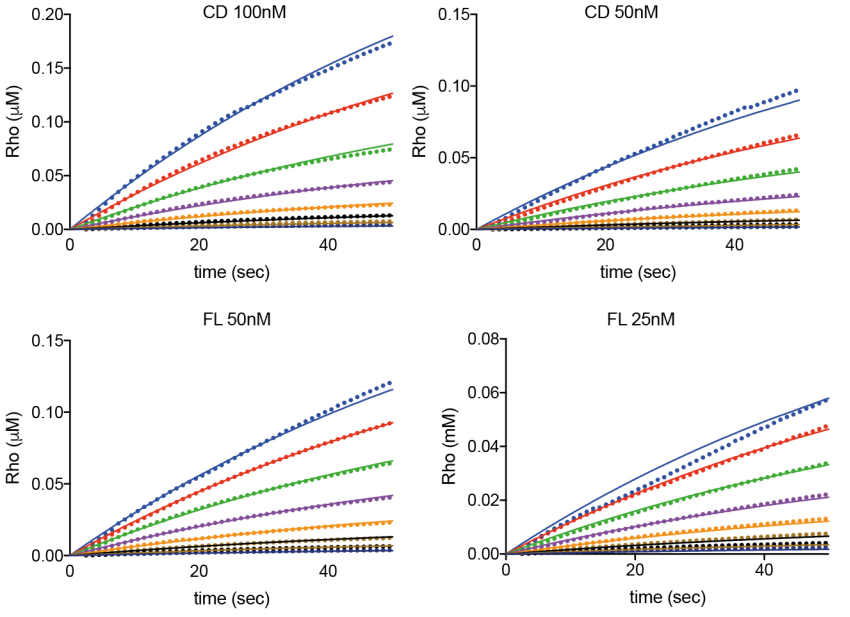

B

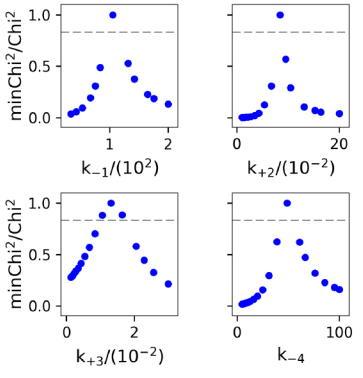

$$ZufspCD + UbRh \underset{k_{-1}}{\overset{k_1}{\rightleftarrows}} ZufspCD \cdot UbRh$$

$$ZufspCD \cdot UbRh \underset{k_{-2}}{\overset{k_2}{\rightleftarrows}} ZufspCD + Rh$$

$$Rh \underset{k_{-3}}{\overset{k_3}{\rightleftarrows}} Rhi$$

$$ZufspFL + UbRh \underset{k_{-4}}{\overset{k_4}{\rightleftarrows}} ZufspFL \cdot UbRh$$

$$ZufspFL \cdot UbRh \underset{k_{-5}}{\overset{k_5}{\rightleftarrows}} ZufspFL + Rh$$

Where

$k_{on}=k_1=k_4=10*\mu M^{-1}*s^{-1}$

$k_{-2}=k_{-3}=k_{-5}=0$

$k_{cat}=k_2=k_5$

k_{on} *is* k_{-1} *and* k_{-4}

C

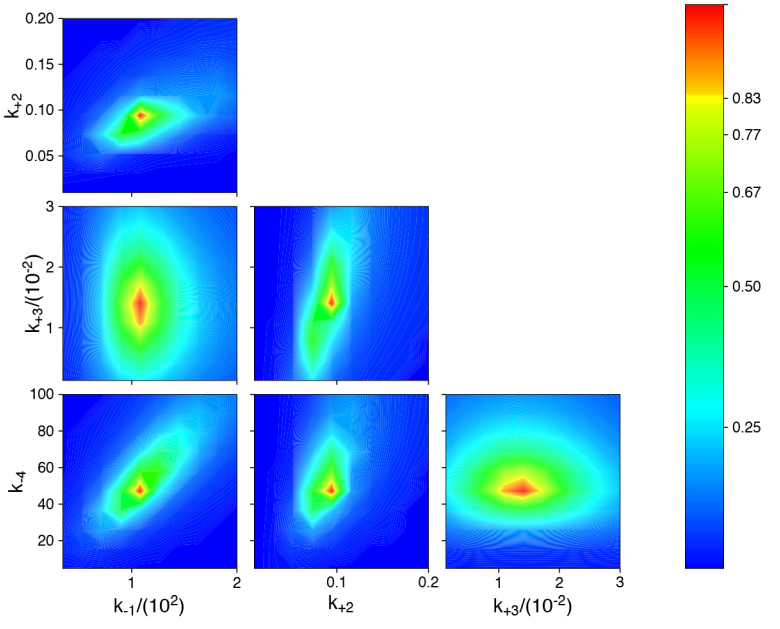

Figure S2. Related to Figure 3

Kinetic modeling of ZUFSP DUB activity

A. Fitting of Ub-Rhodamine kinetic assays by KinTek Explorer to a simple Michaelis-Menten model, with correction for the signal decrease due to the adsorption of free Rhodamine (Rh to Rhi) to well surfaces. The association constant was fixed (k_{on} = 10 $\mu M^{-1}s^{-1}$) to reflect a diffusion-limited process, and reverse reactions were assumed not to be relevant. Joint data fitting for FL and CD at two protein concentrations. Raw data shown as dots and fitted curves as solid line. Initial fitting was performed with individual k_{cat} values (k_2 and k_5). As they refined to equal values, the value was fixed equivalent, and the overall fitting improved. **B**. chi^2 plots for each individual parameter that allow definition of upper and lower boundaries for the parameter. **C**. $Chi^2min/Chi^2x,y$ plots of pair-wise 2-dimensional search. These figures reveal that complex relationships exist between these parameters.

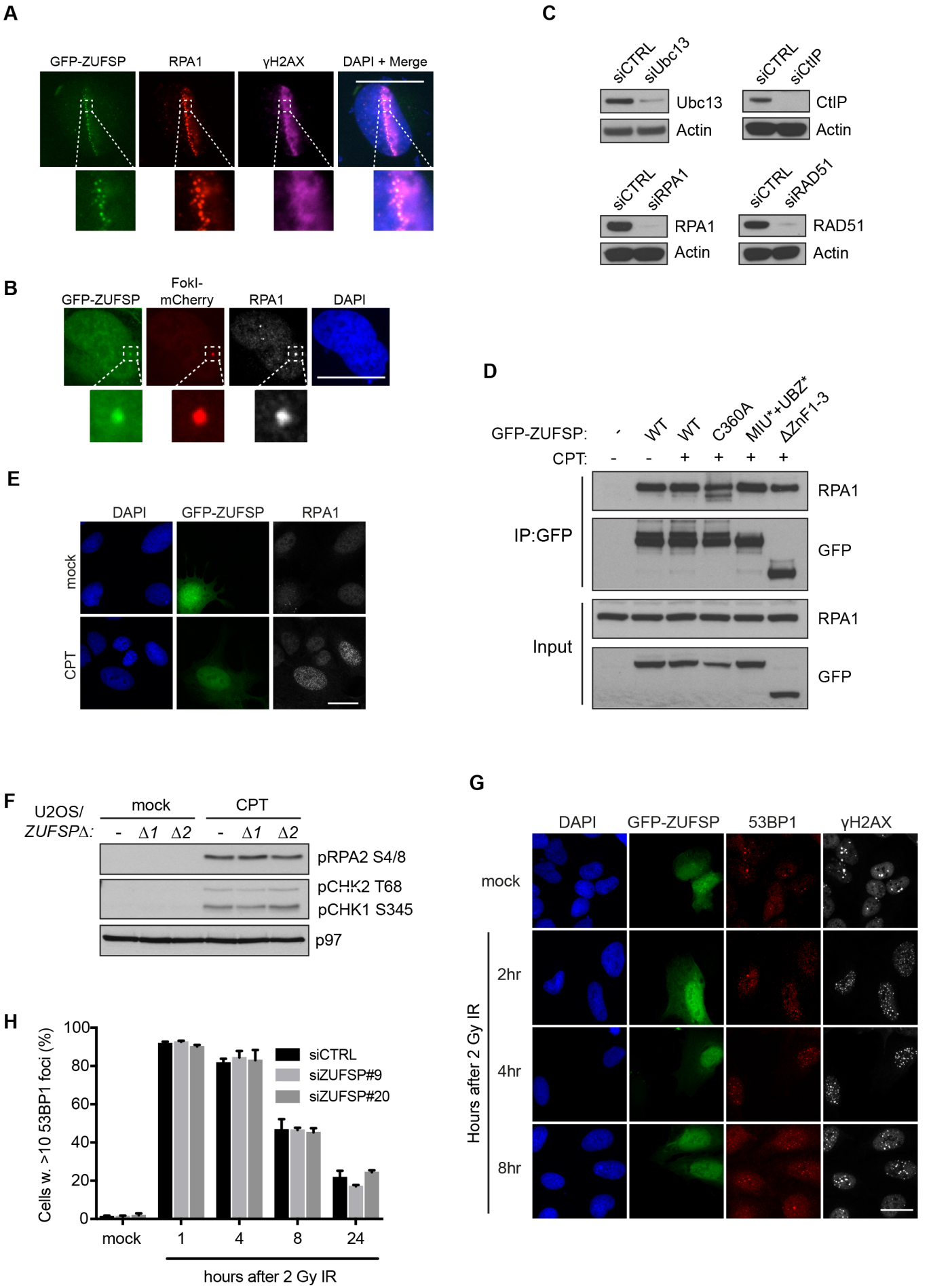
A
GFP-ZUFSP
RPA1
γH2AX
DAPI + Merge
B
GFP-ZUFSP
FokI-mCherry
RPA1
DAPI
C
siCTRL
siUbc13
Ubc13
Actin
siCTRL
siCtIP
CtIP
Actin
siCTRL
siRPA1
RPA1
Actin
siCTRL
siRAD51
RAD51
Actin
D
GFP-ZUFSP:
-
WT
WT
C360A
MIU*+UBZ*
ΔZnF1-3
CPT:
- - + + + +
IP:GFP
RPA1
GFP
Input
RPA1
GFP
E
DAPI
GFP-ZUFSP
RPA1
mock
CPT
F
U2OS/
ZUFSPΔ:
mock
CPT
- Δ1 Δ2 - Δ1 Δ2
pRPA2 S4/8
pCHK2 T68
pCHK1 S345
p97
G
DAPI
GFP-ZUFSP
53BP1
γH2AX
mock
2hr
4hr
8hr
Hours after 2 Gy IR
H
Cells w. >10 53BP1 foci (%)
100
80
60
40
20
0
siCTRL
siZUFSP#9
siZUFSP#20
mock
1
4
8
24
hours after 2 Gy IR

Figure S3. Related to Figure 4

ZUFSP is dispensable for responses to DSBs

A. Representative images showing GFP-ZUFSP co-localization with RPA1 in microfoci in a subset of cells exposed to laser microirradiation-induced DSBs. U2OS cells transiently expressing GFP-ZUFSP were subjected to laser microirradiation. Fifty min later, cells were pre-extracted and co-immunostained with RPA1 and γH2AX antibodies. Scale bar, 10 μm. **B**. U2OS/ER-mCherry-LacR-FokI-DD/LacO cells transfected with GFP-ZUFSP WT plasmid were treated with 4-hydroxytamoxifen and Shield-1 for 5 h to induce clustered DSBs within a single *LacO* genomic locus, then fixed and immunostained with RPA1 antibody. Representative images are shown. Scale bar, 10 μm. **C**. Immunoblot analysis of U2OS/ER-mCherry-LacR-FokI-DD/*LacO* cells transfected with indicated siRNAs. See also Fig. 4B,C. **D**. U2OS cells stably expressing indicated versions of GFP-ZUFSP were treated with camptothecin (CPT, 1 μM) for 2 h and processed for GFP immunoprecipitation followed by immunoblotting with RPA and GFP antibodies. **E**. Representative images of U2OS cells transiently expressing GFP-ZUFSP WT treated with campthothecin (CPT, 1 μM) for 1 h. Cells were then fixed and immunostained with RPA1 antibody. Scale bar, 10 μm. **F**. Immunoblot analysis of U2OS cells (−) or derivative *ZUFSP* knockout (*ZUFSP*Δ) lines treated or not with campthothecin (CPT, 1 μM) for 1 h. See Fig. S4D for immunoblot analysis of ZUFSP expression. **G**. U2OS cells transfected with GFP-ZUFSP WT expression plasmid were subjected to ionizing radiation (IR, 2 Gy) and fixed at the indicated time points. Cells were then co-immunostained with 53BP1 and γ-H2AX antibodies. Representative images are shown. Scale bar, 10 μm. **H**. As in (G), except that U2OS cells were transfected with the indicated siRNAs prior to IR treatment. Proportion of cells containing >10 53BP1 foci was determined (mean±SEM; 150-200 cells quantified per condition per experiment; *n*=2 independent experiments).

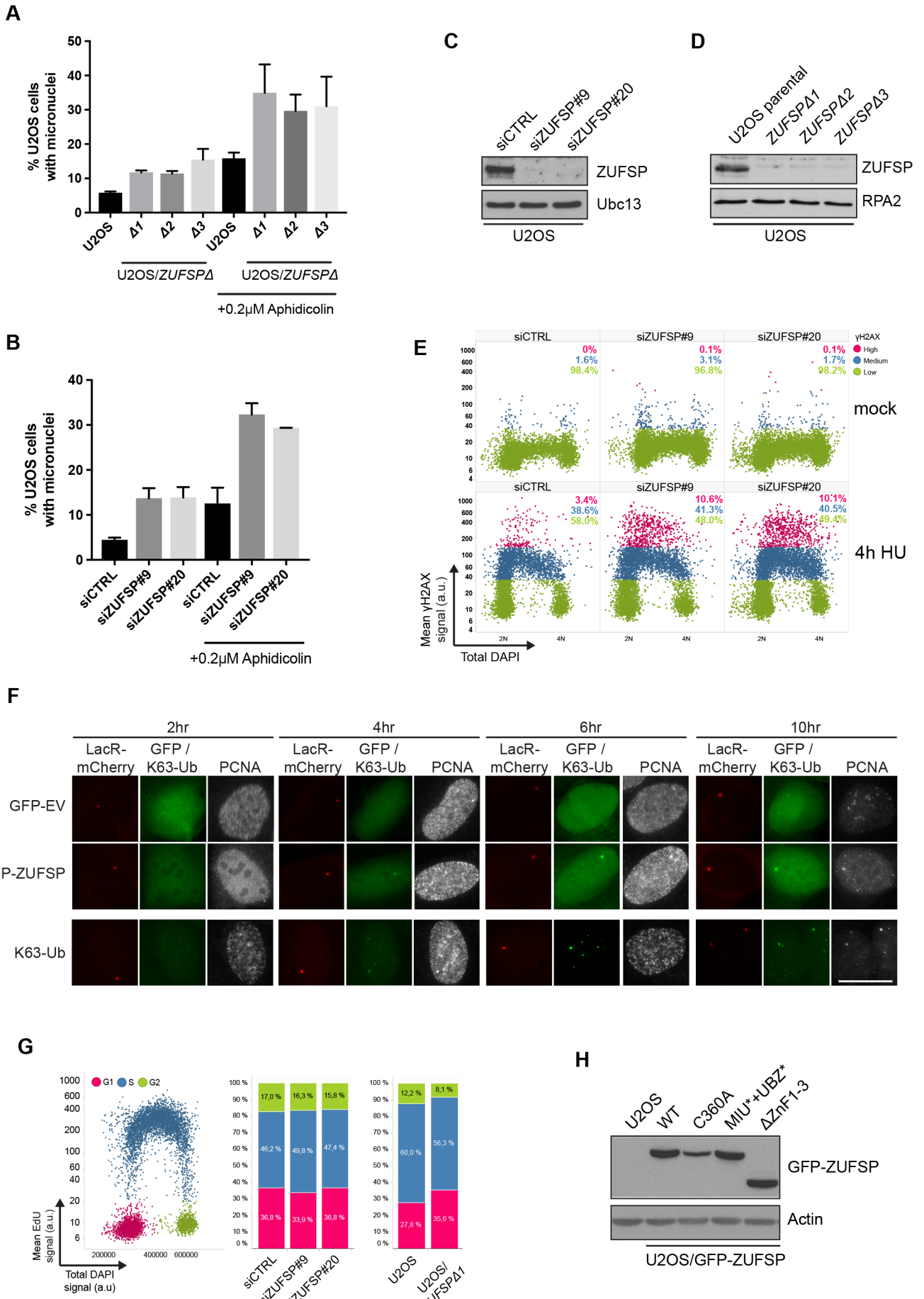
A
% U2OS cells with micronuclei
U2OS
Δ1
Δ2
Δ3
U2OS/ZUFSPΔ
+0.2μM Aphidicolin
B
% U2OS cells with micronuclei
siCTRL
siZUFSP#9
siZUFSP#20
+0.2μM Aphidicolin
C
siCTRL
siZUFSP#9
siZUFSP#20
ZUFSP
Ubc13
U2OS
D
U2OS parental
ZUFSPΔ1
ZUFSPΔ2
ZUFSPΔ3
ZUFSP
RPA2
U2OS
E
siCTRL
siZUFSP#9
siZUFSP#20
γH2AX
High
Medium
Low
mock
4h HU
Mean γH2AX signal (a.u.)
Total DAPI
2N
4N
F
2hr
4hr
6hr
10hr
LacR-mCherry
GFP / K63-Ub
PCNA
GFP-EV
GFP-ZUFSP
K63-Ub
G
G1
S
G2
Mean EdU signal (a.u.)
Total DAPI signal (a.u)
siCTRL
siZUFSP#9
siZUFSP#20
U2OS
U2OS/ ZUFSPΔ1
H
U2OS WT
C360A
MIU*+UBZ*
ΔZnF1-3
GFP-ZUFSP
Actin
U2OS/GFP-ZUFSP

Figure S4. Related to Figure 4

ZUFSP functions in the replication stress response

A. U2OS cells or derivative *ZUFSP* knockout (*ZUFSP*Δ) lines were treated or not with aphidicolin (0.2 μM) for 24 h, then fixed and stained with DAPI. Proportion of cells with micronuclei was determined (mean±SEM; 400 cells quantified per condition; *n*=2 independent experiments). See also Fig. S4D. **B**. U2OS cells transfected with indicated ZUFSP siRNAs were treated and processed as in (A) (mean±SEM; 400 cells quantified per condition; *n*=2-4 independent experiments). See also Fig. S4C. **C**. Immunoblot analysis of U2OS cells transfected with control siRNA (siCTRL) or siRNAs targeting ZUFSP for 48 h. **D**. Immunoblot analysis of parental U2OS cells and derivative *ZUFSP* knockout (*ZUFSP*Δ) lines. **E**. U2OS cells treated with indicated siRNAs were treated with HU (2 mM) for 4 h, fixed and immunostained with γ-H2AX antibody in the presence of DAPI, and analyzed by high content microscopy. Proportion of cells with low (green), medium (blue) and high (pink) γ-H2AX signal is indicated. At least 4000 cells were analyzed per condition. Data from a representative experiment are shown. **F**. Representative images of U2OS/2-6-3 cells carrying a single *LacO* array (white arrow) that were synchronized at the G1/S border by a double thymidine block, transfected with constructs encoding GFP-ZUFSP or GFP empty vector (EV), then released into S phase for the indicated times in the presence of LacR-mCherry expression and fixed and immunostained with PCNA antibody. In the lower panel, cells were additionally pre-extracted and co-immunostained with K63-Ub antibody. Scale bar, 10 μm. **G**. Quantitative image analysis of asynchronously growing U2OS cells and U2OS cells depleted of ZUFSP that were labelled with EdU and stained with DAPI (*n*=2000 cells per condition). The proportion of cells in different cell cycle phases (pink: G1 phase; blue: S phase; green: G2/M phase) is indicated. **H**. Immunoblot analysis of U2OS cells or derivative cell lines stably expressing the indicated GFP-ZUFSP transgenes.